University of Minnesota
Driven to Discover

U.S. DEPARTMENT OF ENERGY

Magnetic order in hyperhoneycomb magnet β-Li_2IrO_3 and its evolution in magnetic field

Natalia Perkins

University of Minnesota

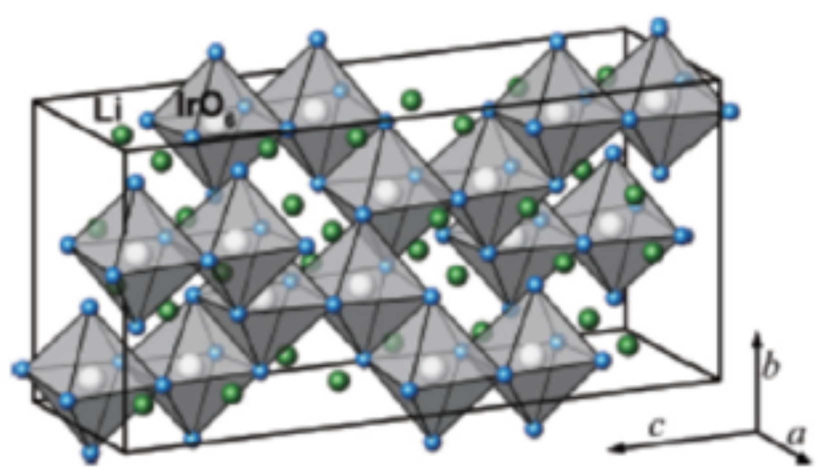

IBSPCS-KIAS International Workshop Frustrated Magnetis
October 15, 2019

Collaborators

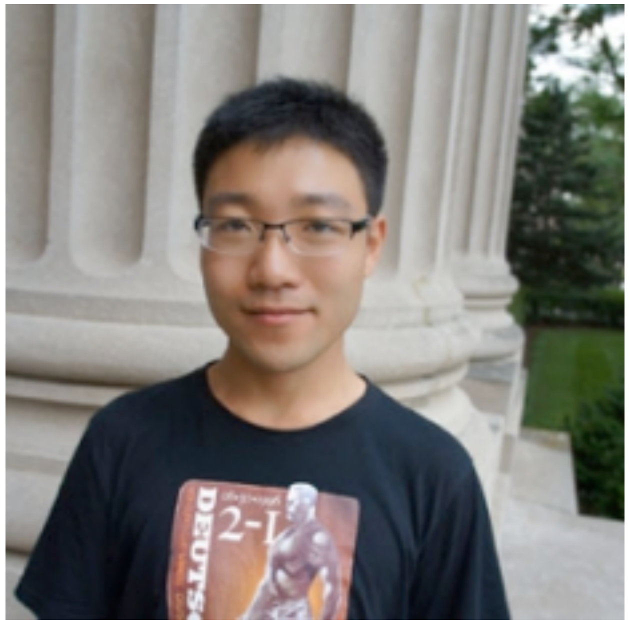

Mengqun Li
UMN

Ioannis Rousochatzakis
Loughborough University (UK)

Everything started with the model ...

A. Kitaev, Annals of Physics **321**, 2 (2006)

$$H = -\sum_{x-bonds} J_x \sigma_j^x \sigma_k^x - \sum_{y-bonds} J_y \sigma_j^y \sigma_k^y - \sum_{z-bonds} J_z \sigma_j^z \sigma_k^z$$

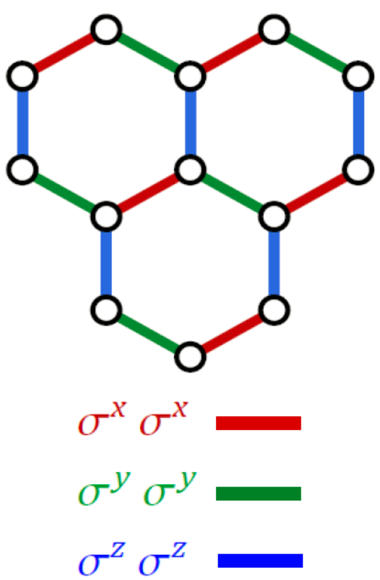

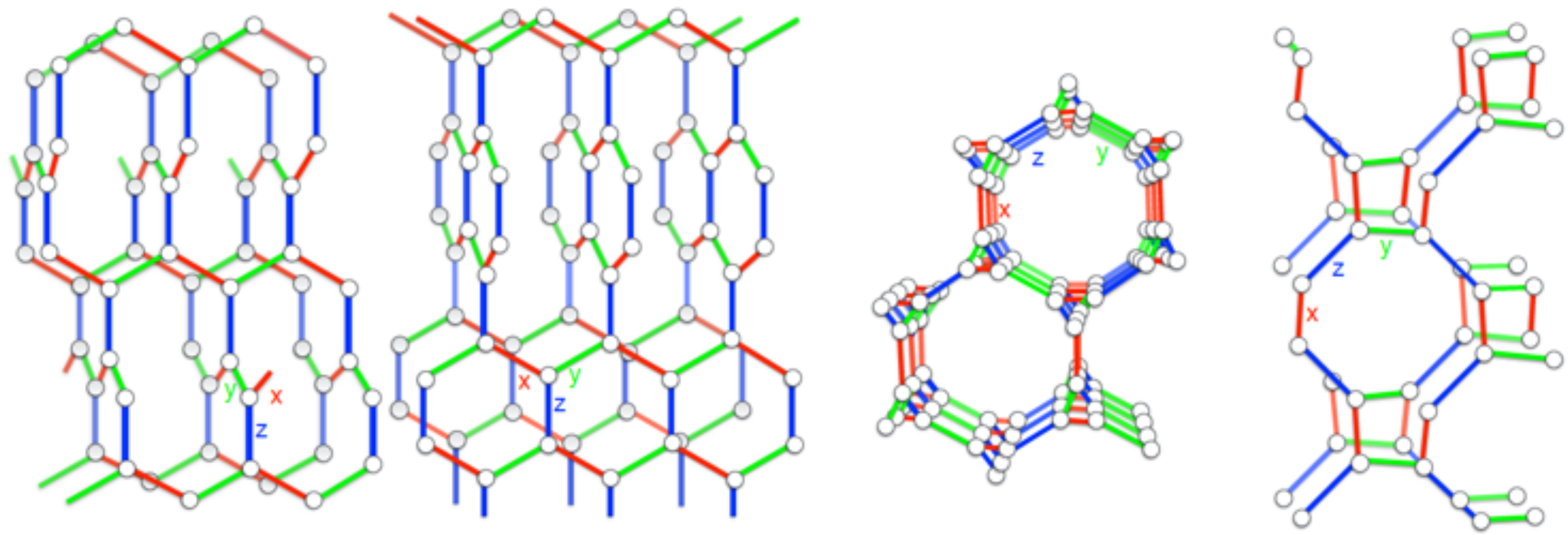

(a) hyper-honeycomb (b) stripy-honeycomb (c) hyper-hexagon (d) hyper-octagon

Exactly solvable

Spin liquid ground state

The Kitaev model *appeared to be realizable …*

G. Jackeli and G. Khaliullin,
PRL 102, 017205 (2009)

Ir^{4+} - $5d^5$
Rh^{4+} - $4d^5$
Ru^{3+} - $4d^5$

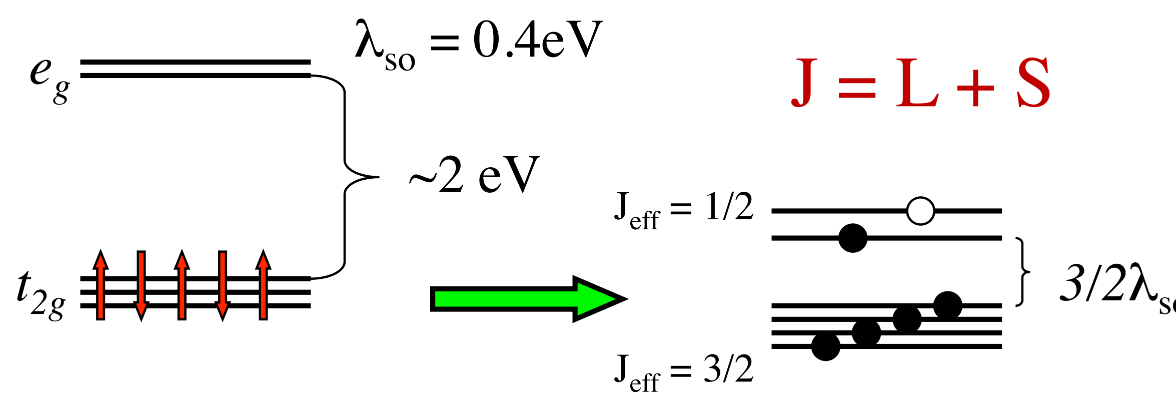

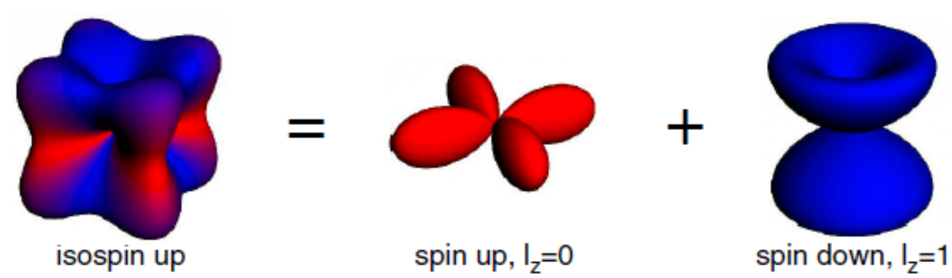

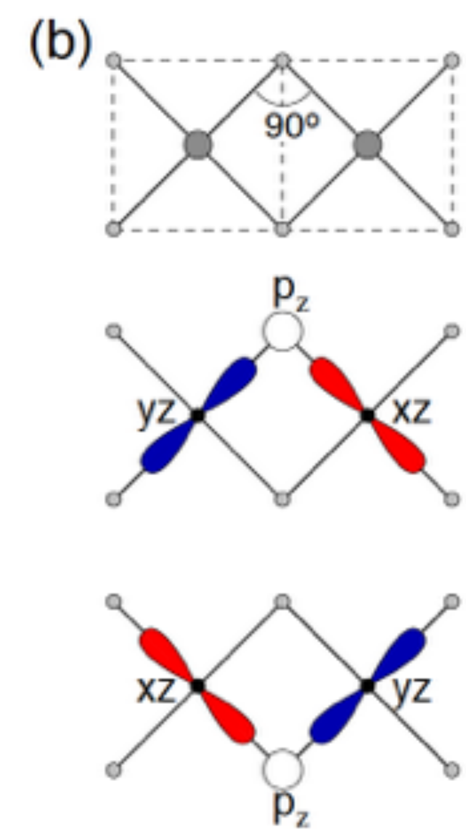

Effective low-energy Hamiltonian for J_{eff} = 1/2 ”spins”:

$$H = H_K + \text{(other terms)}$$

Experimental realizations in 2D

Na_2IrO_3
alpha-Li_2IrO_3

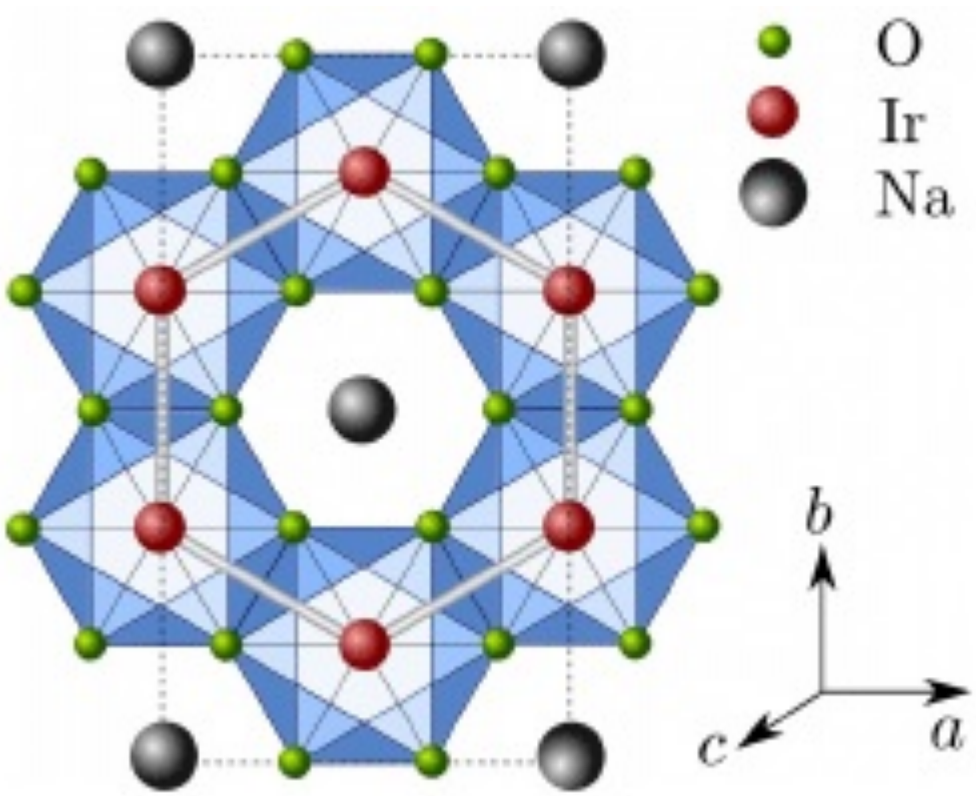

Y.Singh, P. Gegenwart, PRL 2010, 2011

alpha-$RuCl_3$

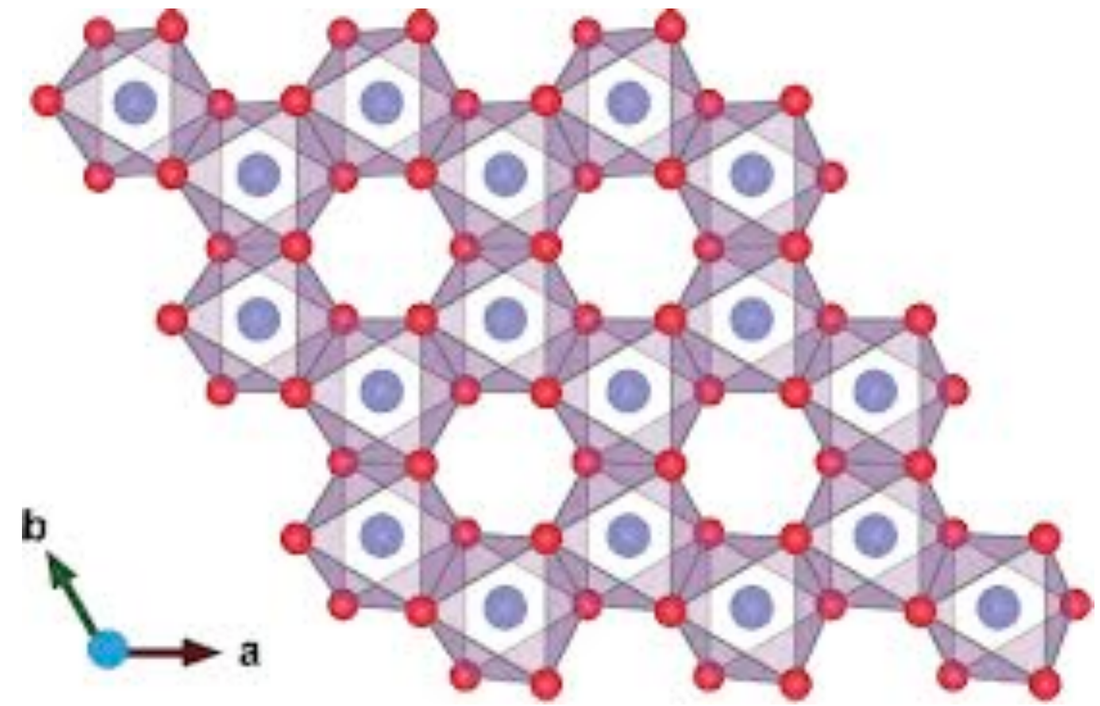

K. Plumb et al, Phys. Rev. B (2014)
A. Banerjee et al, Nature Materials (2016)

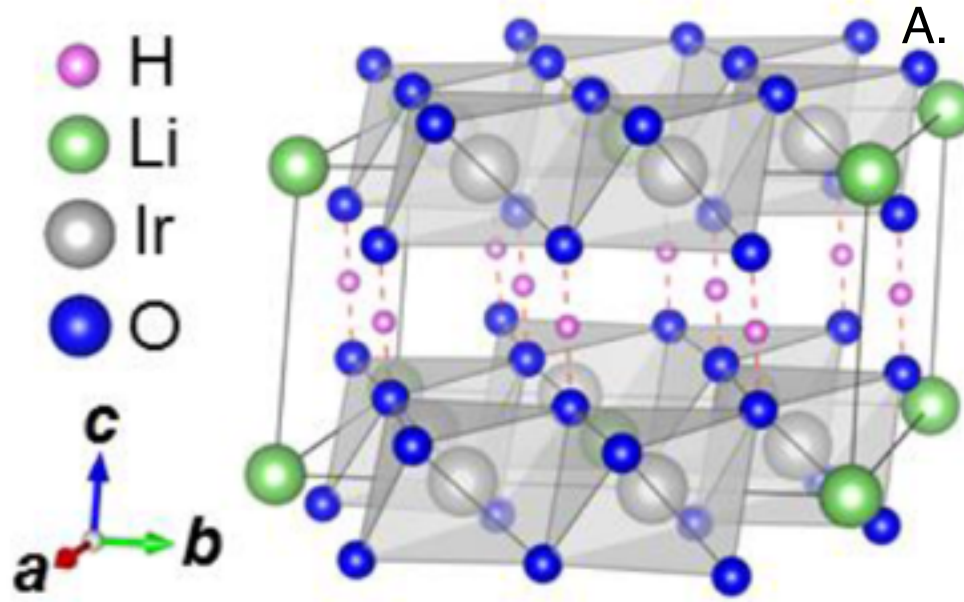

$H_3LiIr_2O_6$

Kitagawa et al, Nature(2018)

Experimental realizations in 3D

β-Li_2IrO_3

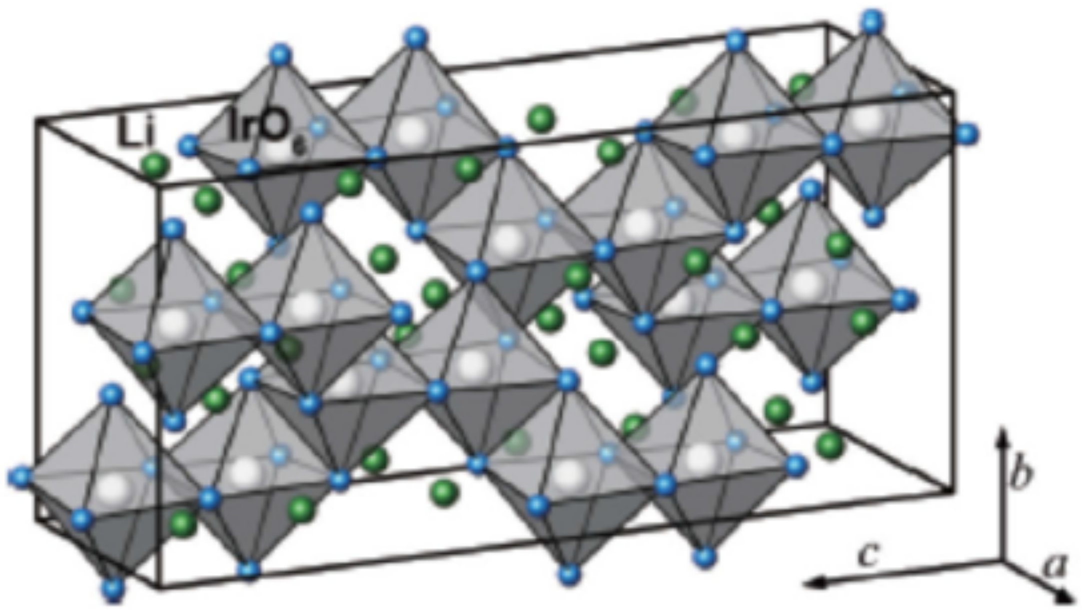

A. Biffin et al, PRB (2014)

T. Takayama et al, PRL (2015)

γ-Li_2IrO_3

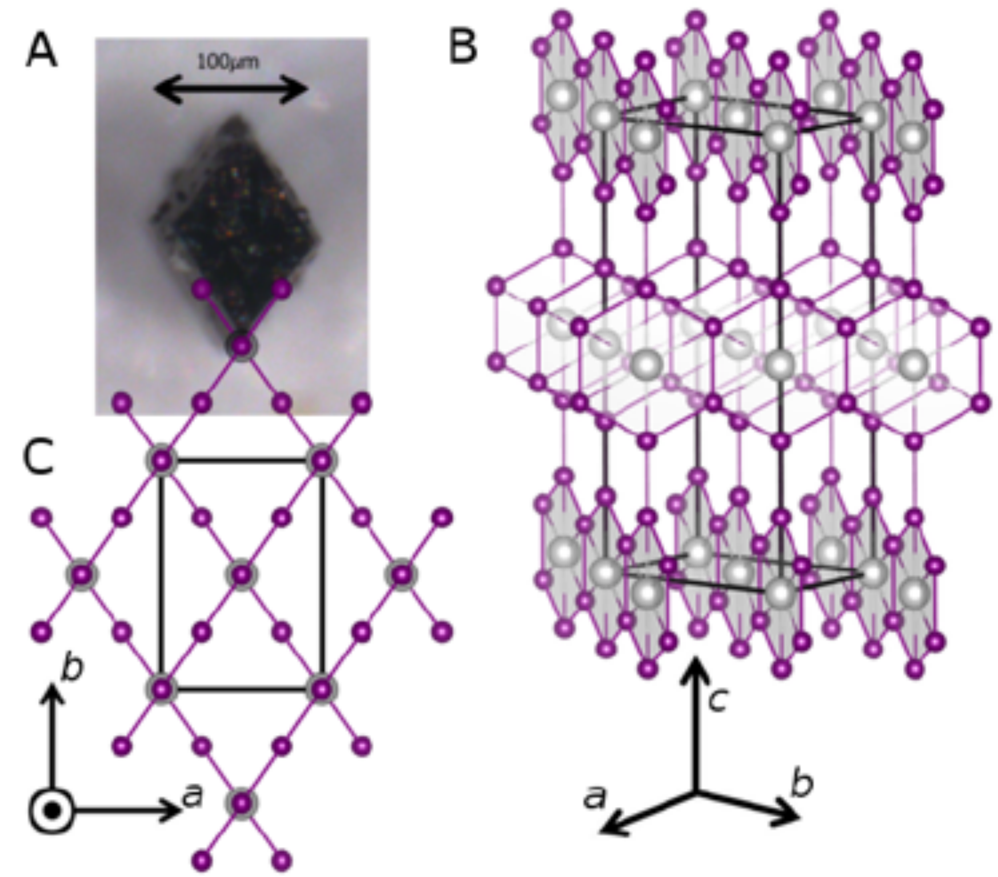

Modic et al, Nature Comm. (2014)

A. Biffin et al, PRL (2014)

Physics is different from pure Kitaev spin liquid but very interesting

$H = H_K$ + (other terms)

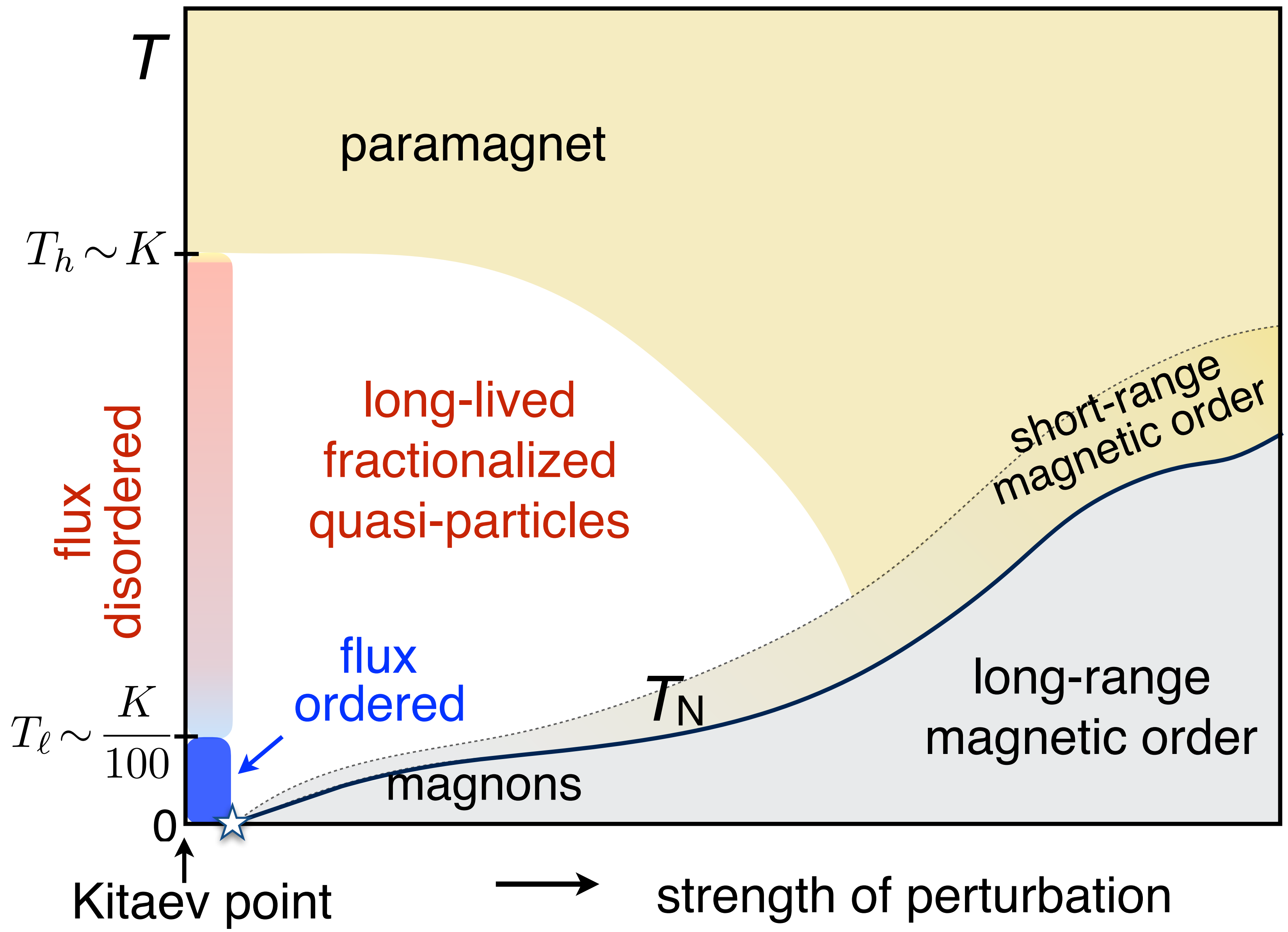

I. Rousochatzakis, S. Kourtis, J. Knolle, R. Moessner, **NBP,** PRB 2019

Complex magnetism in β-Li_2IrO_3 in applied magnetic field

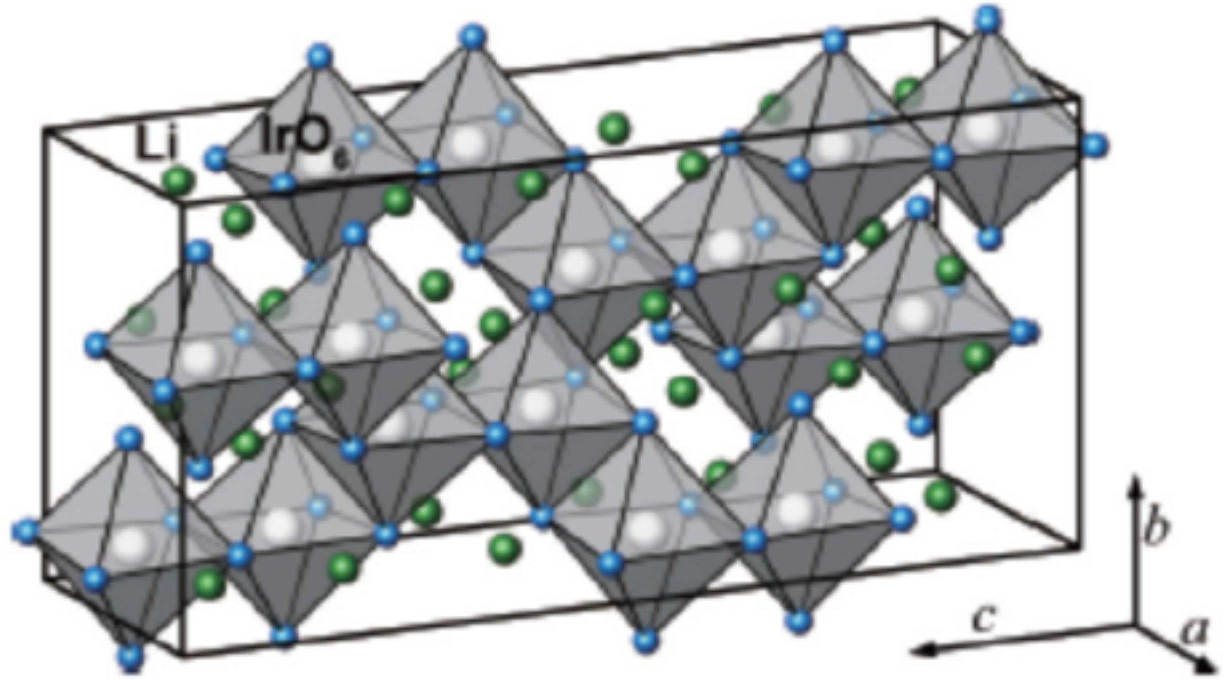

Experiment:

A. Biffin et al, PRB (2014)

T. Takayama et al, PRL (2015)

A. Ruiz et al, Nat.Com. (2017)

L.S.I. Veiga et al, PRB (2017)

M. Majumder et al, PRL (2018), PRM (2019), arXiv:1910.03251

A. Ruiz et al, arXiv:1909.06355

Theory:

E. K.-H. Lee and Y. B. Kim, PRB (2015)

E. K.-H. Lee, J. G Rau and Y. B. Kim, PRB (2015)

I. Kimchi, R. Coldea, and A. Vishwanath, PRB (2015)

I. Kimchi and R. Coldea, PRB (2016)

P. P. Stavropoulos, A. Catuneanu, H.-Y. Kee, PRB (2018)

S. Ducatman, I.Rousochatzakis and **N.P.**, PRB (2018)

I.Rousochatzakis and **N.P.**, PRB (2018)

M. Lee,I.Rousochatzakis and N.P., arxiv:1910.****

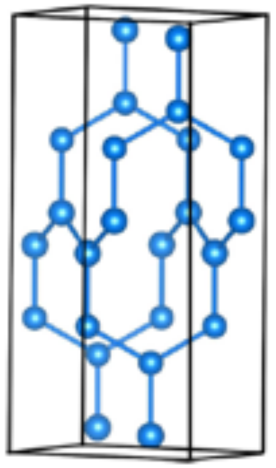

Experimental facts: zero field

T_N=37 K: incommensurate (IC) counter-rotating spiral

β-Li_2IrO_3

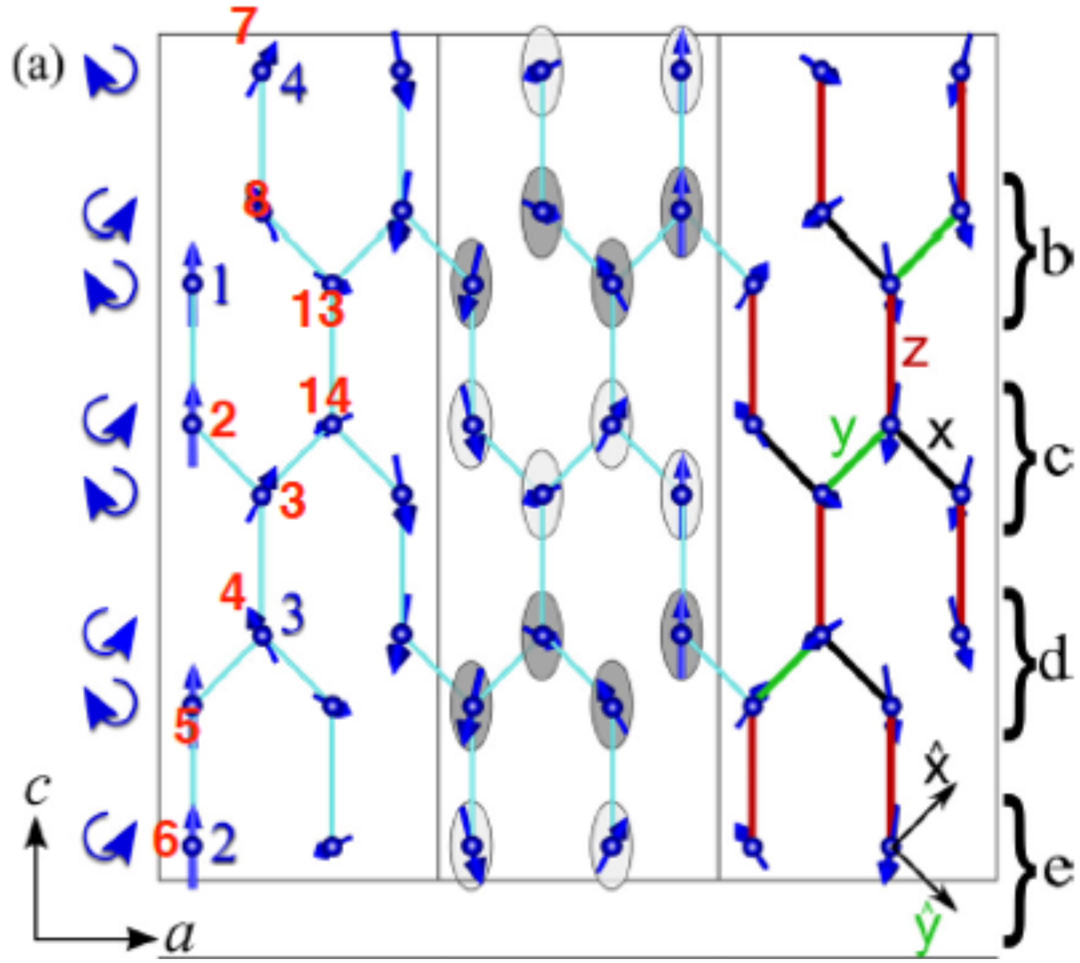

Q=(0.57,0,0)

Irreducible representation: $\mathbf{M}_{(0.57,0,0)} = (iM_aA,\, iM_bC,\, M_cF)$

$$F = \begin{bmatrix} 1 \\ 1 \\ 1 \\ 1 \end{bmatrix},\ A = \begin{bmatrix} 1 \\ -1 \\ -1 \\ 1 \end{bmatrix},\ C = \begin{bmatrix} 1 \\ 1 \\ -1 \\ -1 \end{bmatrix}$$

A. Biffin et al, PRB (2014)

Experimental facts: magnetic field along **b**

Fate of the IC order (very fragile)

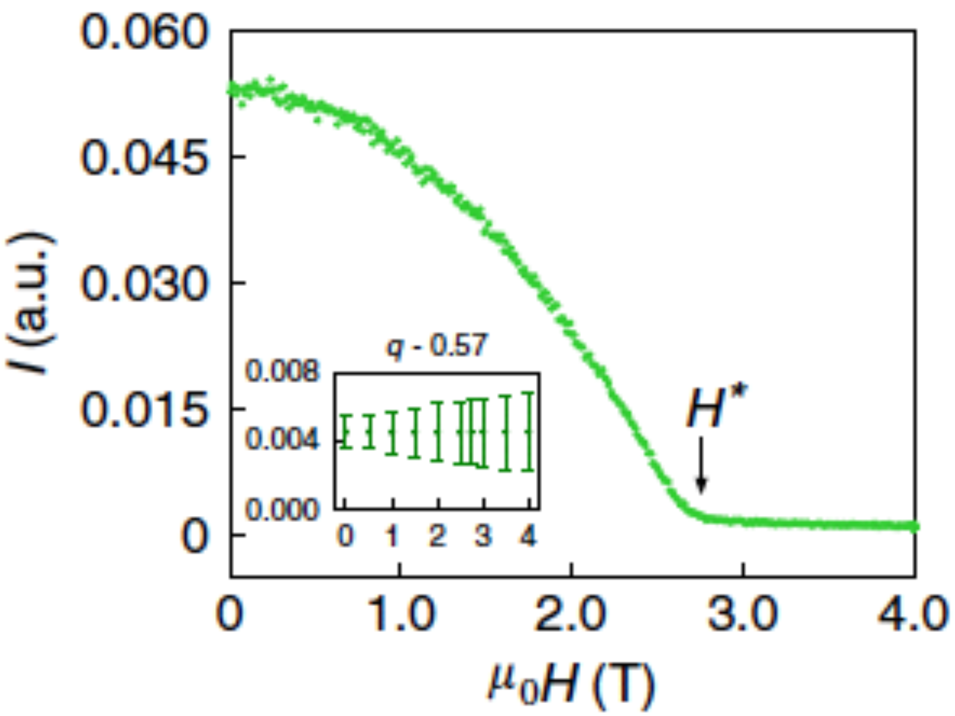

Intensity sum rule

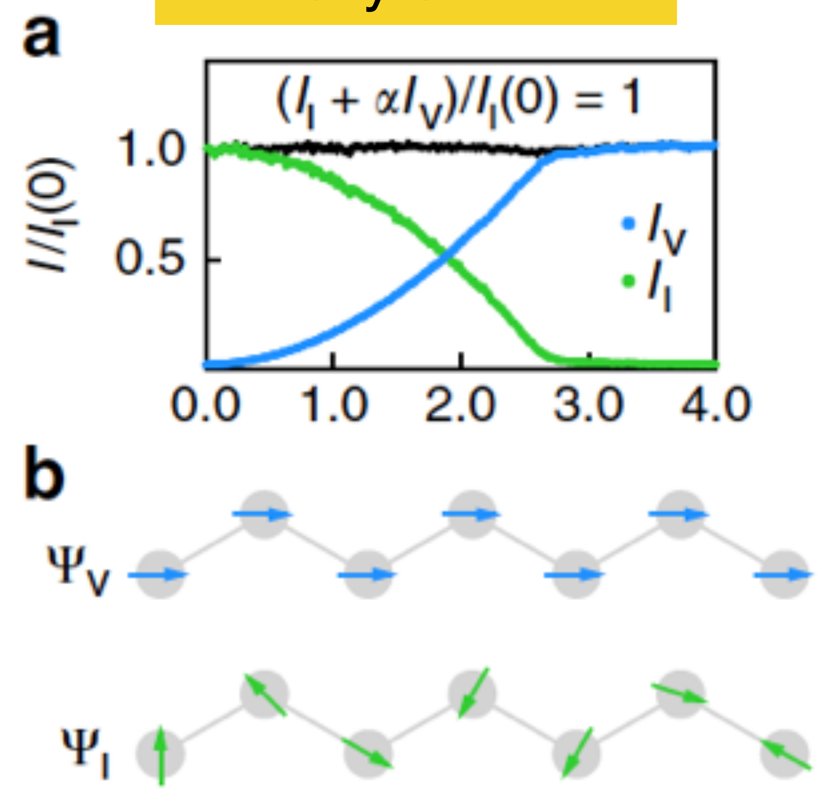

Q=0 order

IC order

The system develops a significant uniform ‘zigzag’ component along **a**

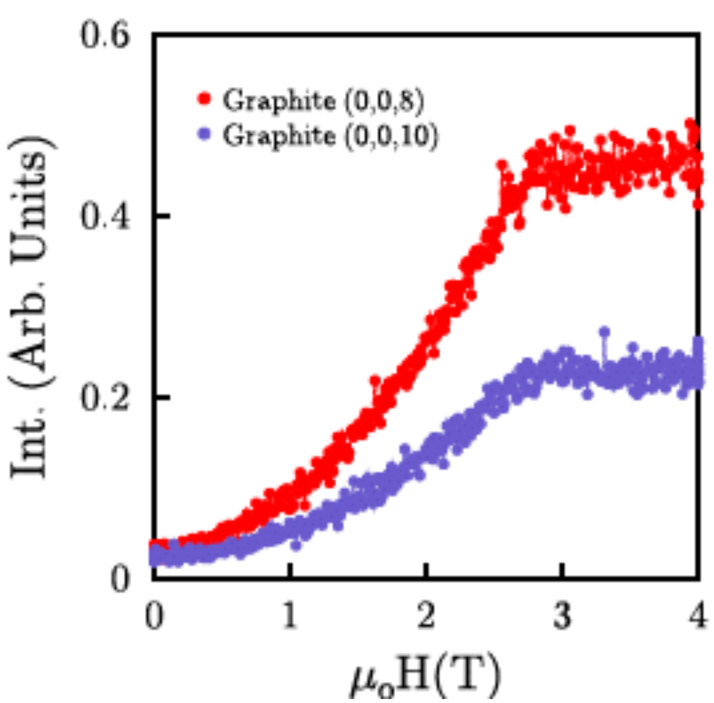

moments along **a**

π-σ channel

moments along **b**

π-π channel

A. Ruiz et al, Nat.Com. 2017

Magnetization vs. magnetic field

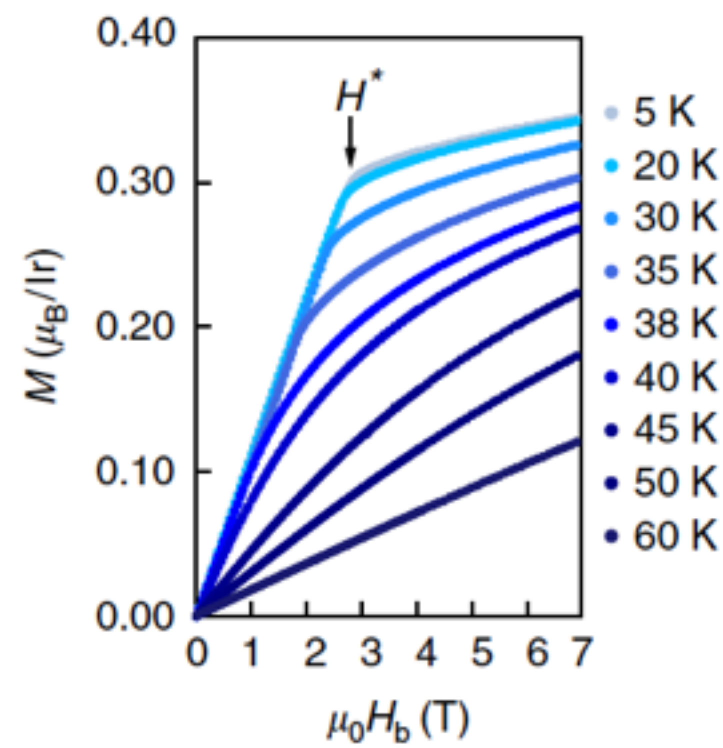

Experimental facts: magnetic field along **a, b** and **c**

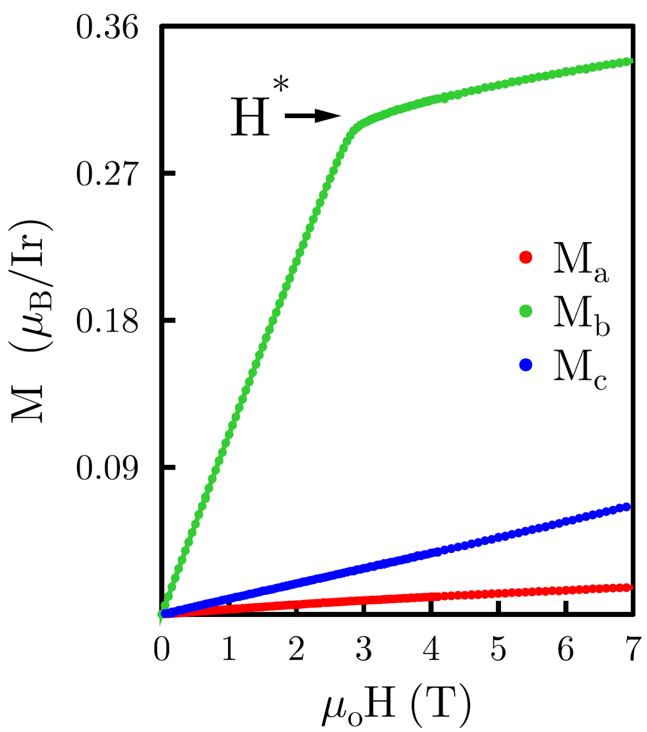

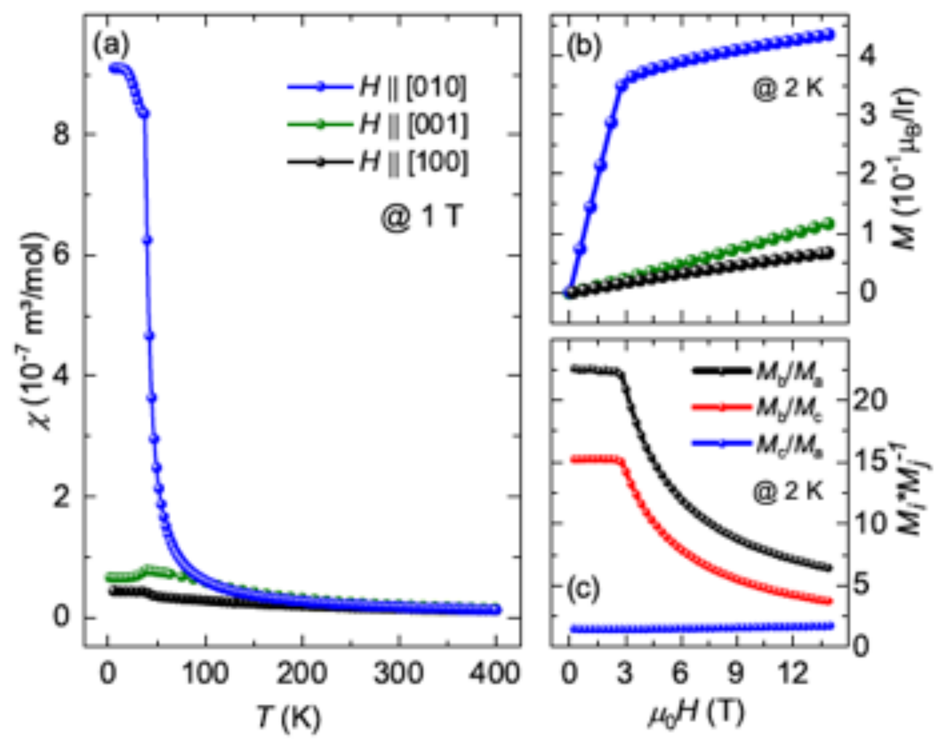

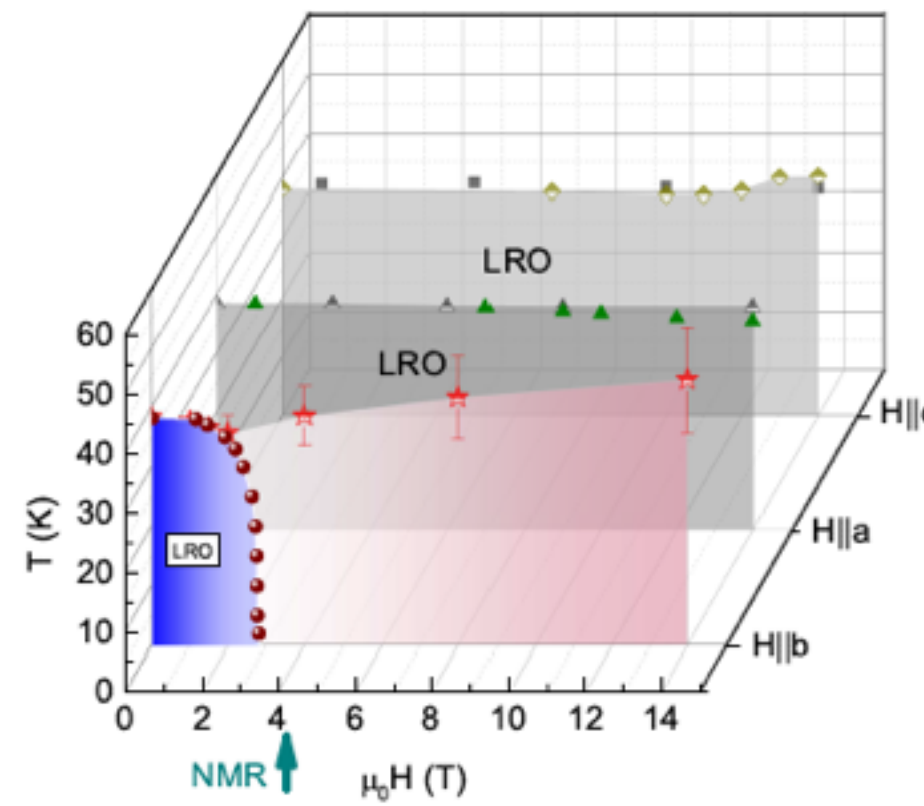

A. Ruiz et al, Nat.Com. 2017

M. Majumder, et al PRM 2019

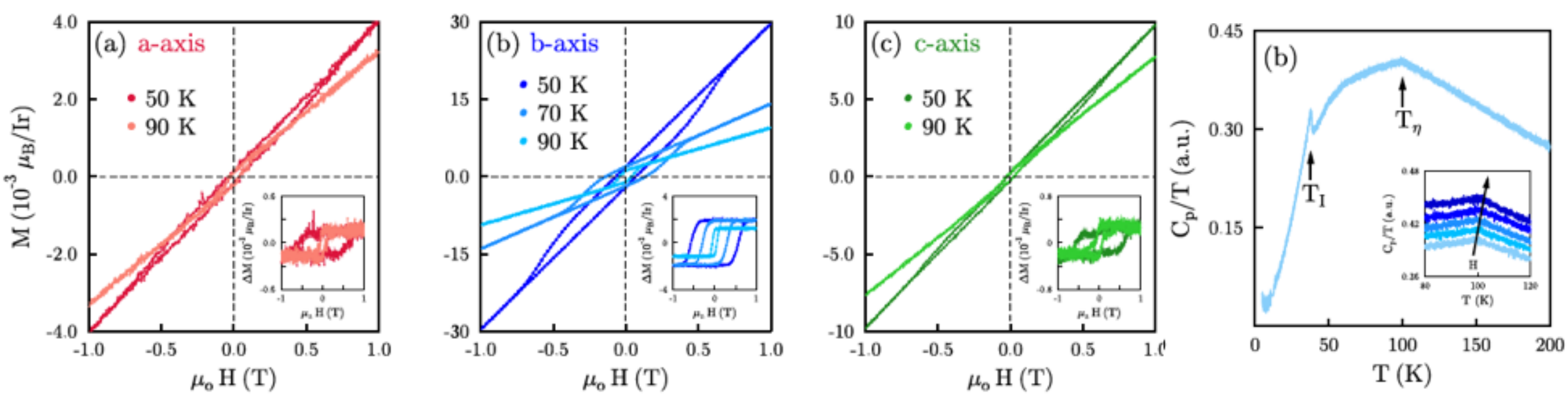

A. Ruiz et al, arXiv:1909.06355

J-*K*-*Γ* model

$$\mathcal{H} = \sum_t \sum_{\langle ij \rangle \in t} \mathcal{H}_{ij}^t$$

$$\mathcal{H}_{ij}^t = J\mathbf{S}_i \cdot \mathbf{S}_j + KS_i^{\alpha_t} S_j^{\alpha_t} + \sigma_t \Gamma (S_i^{\beta_t} S_j^{\gamma_t} + S_i^{\gamma_t} S_j^{\beta_t})$$

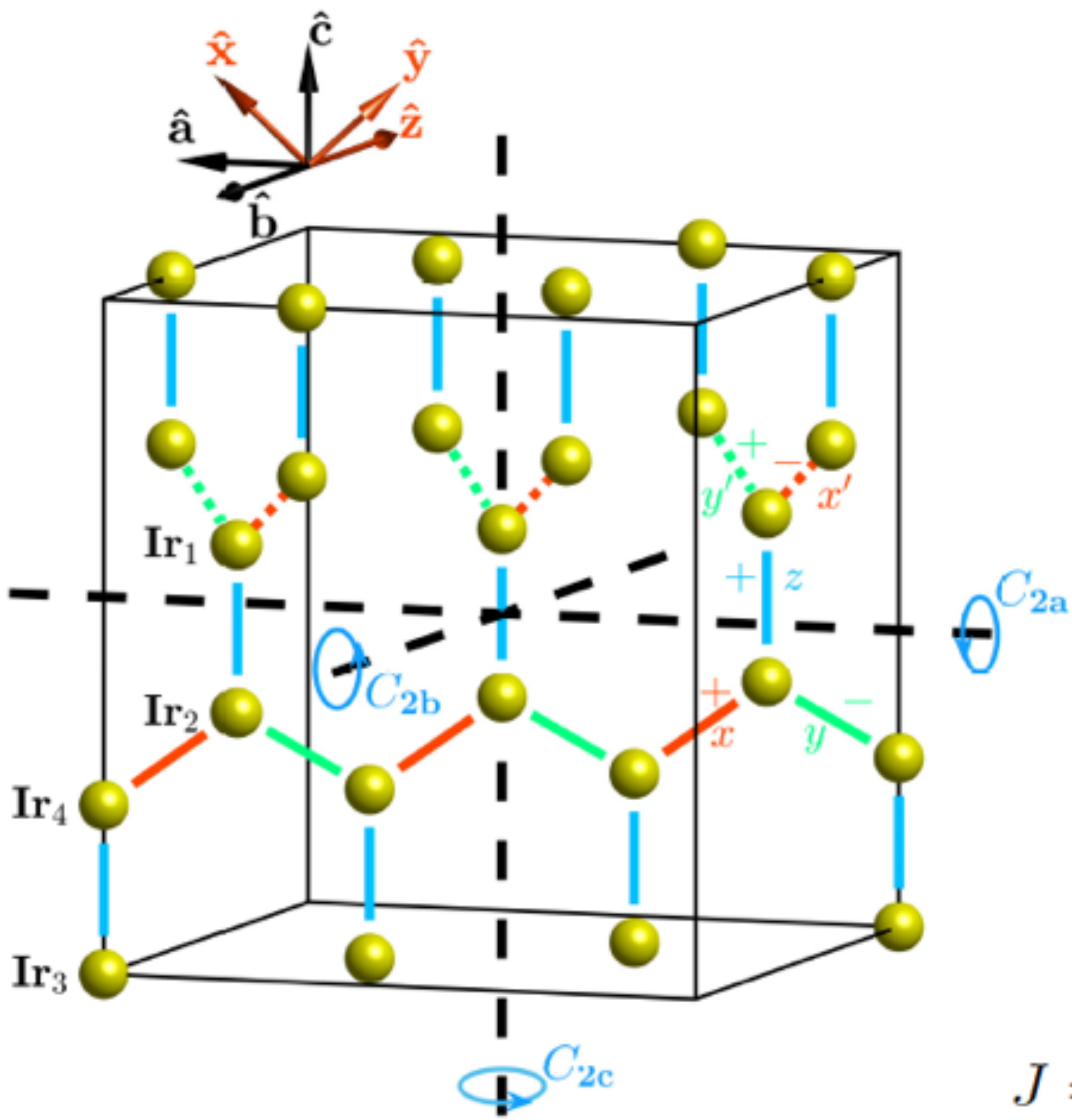

$\hat{\mathbf{x}} = (\hat{\mathbf{a}} + \hat{\mathbf{c}})/\sqrt{2}, \;\; \hat{\mathbf{y}} = (\hat{\mathbf{c}} - \hat{\mathbf{a}})/\sqrt{2}, \;\; \hat{\mathbf{z}} = -\hat{\mathbf{b}}$

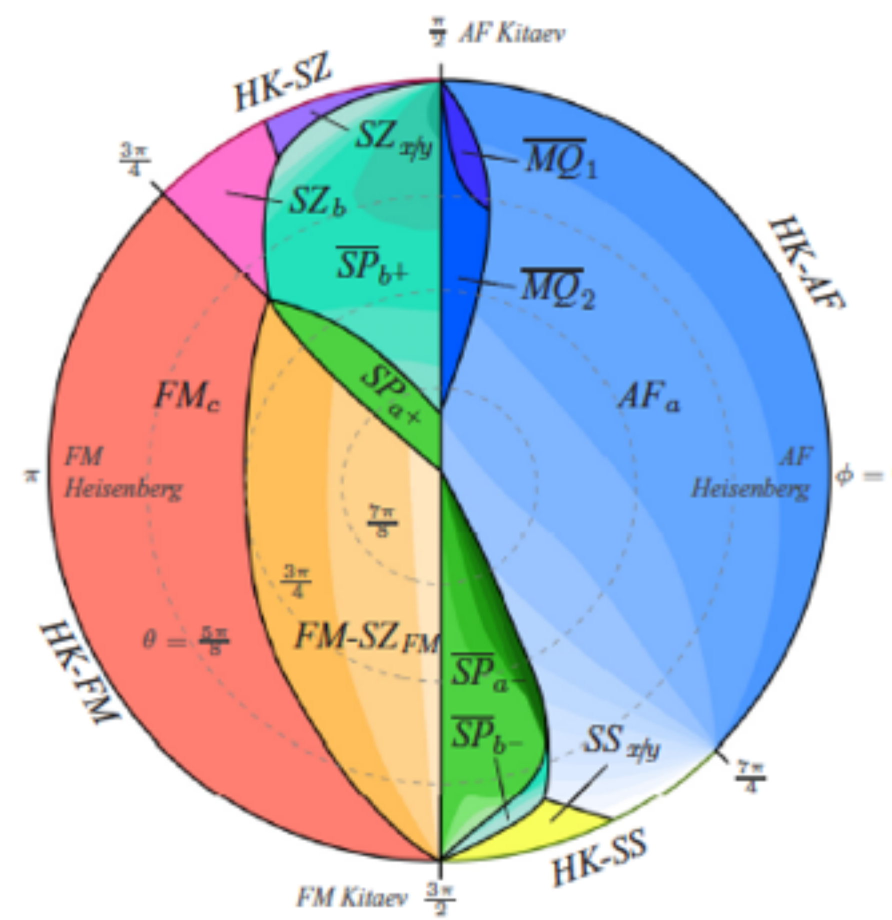

$J = \sin r \cos\phi, \;\; K = \sin r \sin\phi, \;\; \Gamma = \mathrm{sgn}(\Gamma)\cos r$

Eric Kin-Ho Lee and Yong Baek Kim, PRB 2015

J-K-Γ model

$$\mathcal{H} = \sum_{t} \sum_{\langle ij \rangle \in t} \mathcal{H}_{ij}^{t}$$

$$\mathcal{H}_{ij}^{t} = J\mathbf{S}_i \cdot \mathbf{S}_j + K S_i^{\alpha_t} S_j^{\alpha_t} + \sigma_t \Gamma (S_i^{\beta_t} S_j^{\gamma_t} + S_i^{\gamma_t} S_j^{\beta_t})$$

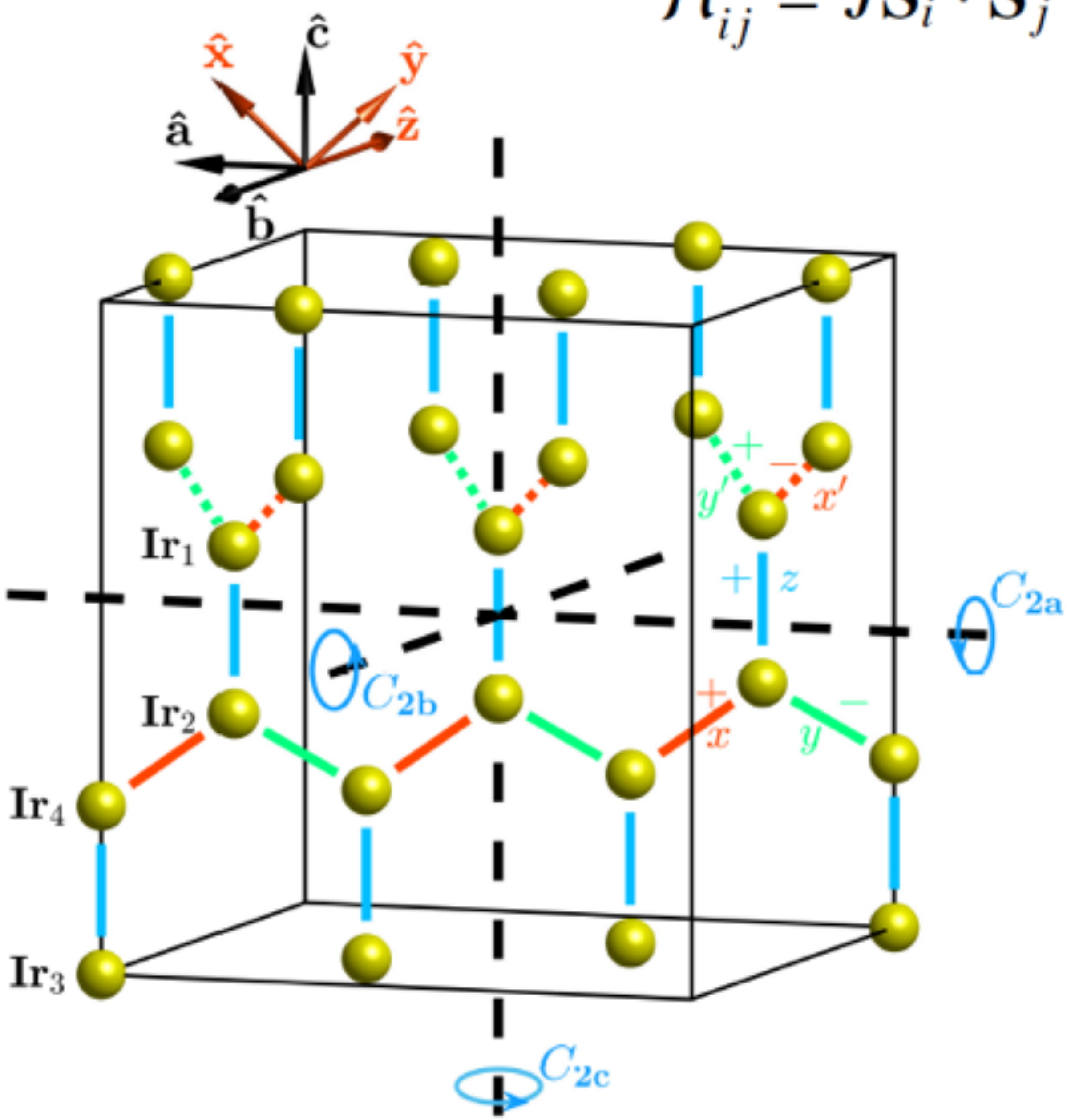

$$\hat{\mathbf{x}} = (\hat{\mathbf{a}} + \hat{\mathbf{c}})/\sqrt{2}, \quad \hat{\mathbf{y}} = (\hat{\mathbf{c}} - \hat{\mathbf{a}})/\sqrt{2}, \quad \hat{\mathbf{z}} = -\hat{\mathbf{b}}$$

$\mathbf{Q} = 2\pi h \hat{\mathbf{a}}$

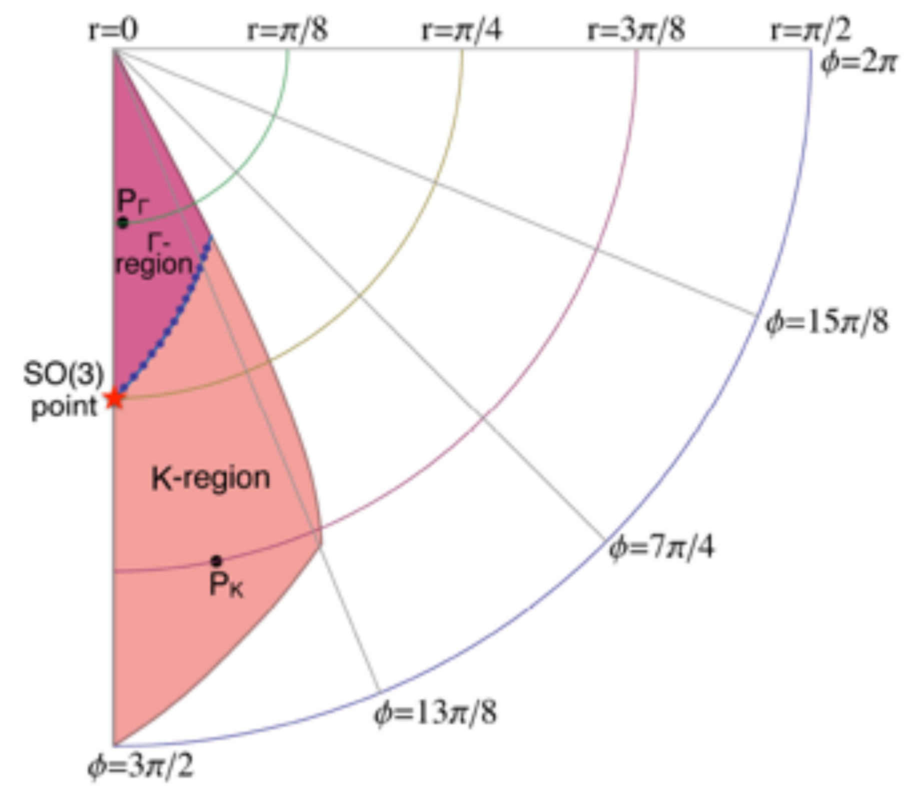

$K < 0, \Gamma < 0, J > 0$

S. Ducatman, I.Rousochatzakis and **N.P.**, PRB (2018)

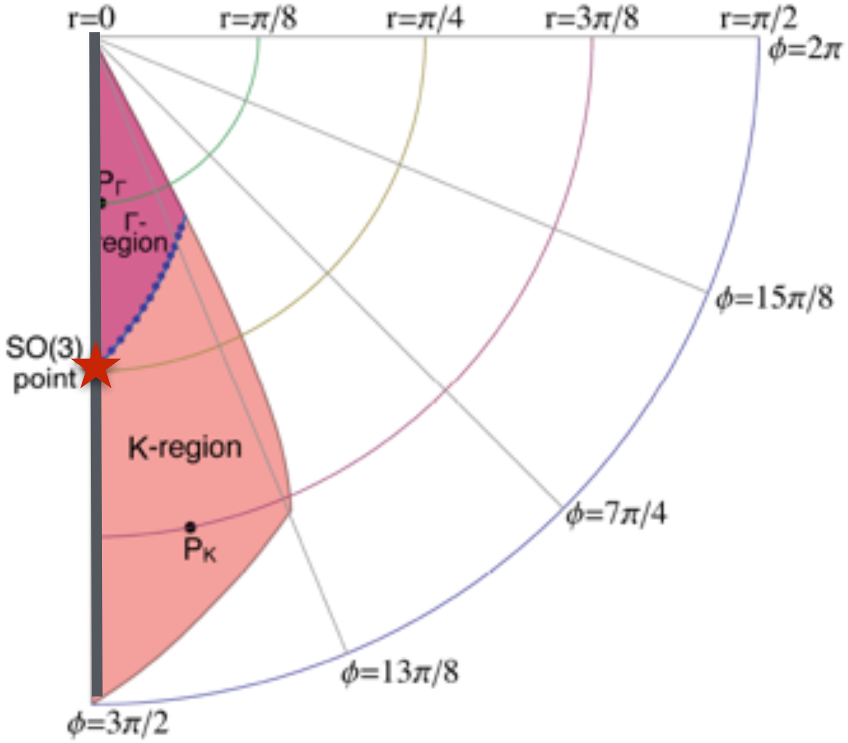

The special line $\phi = 3\pi/2$

$$J = 0$$

$$\mathbf{S}_2 = [-Z_0, Y_0, -X_0]$$

$$\mathbf{S}_3 = [Y_0, X_0, Z_0]$$

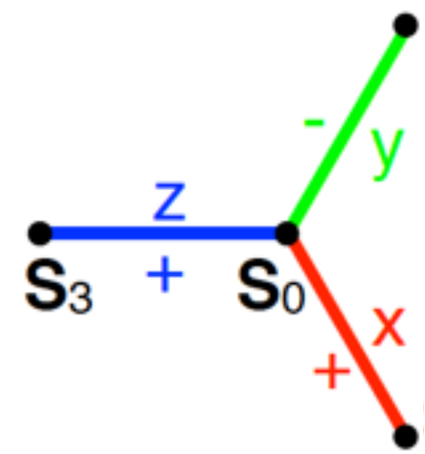

$$\mathbf{S}_1 = [X_0, Z_0, Y_0]$$

$$\Gamma(S_0^y S_1^z + S_0^z S_1^y) + K S_0^x S_1^x$$

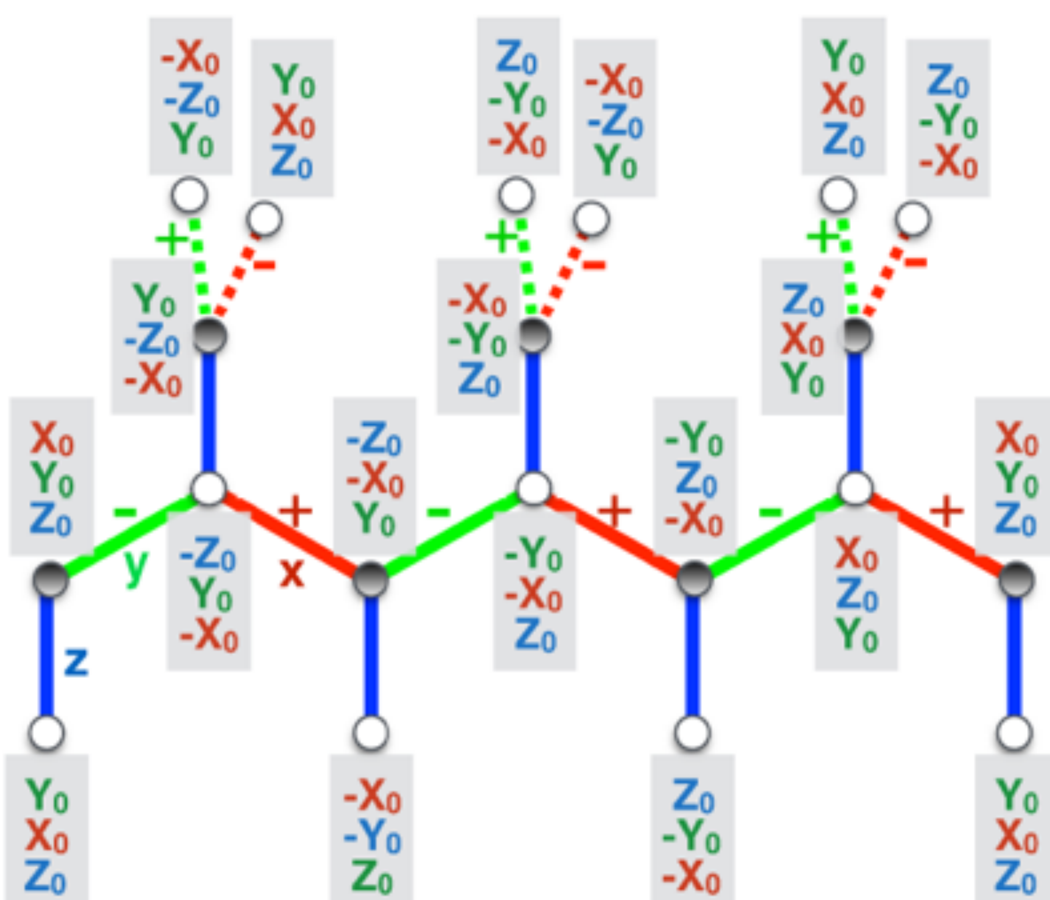

$$E/N = \tfrac{1}{2}(K + 2\Gamma)S^2$$

coincides with min of energy from LT

Classical degeneracy associated with the direction of the initial central spin S_0

S. Ducatman, I. Rousochatzakis and **N.P.**, PRB 2018

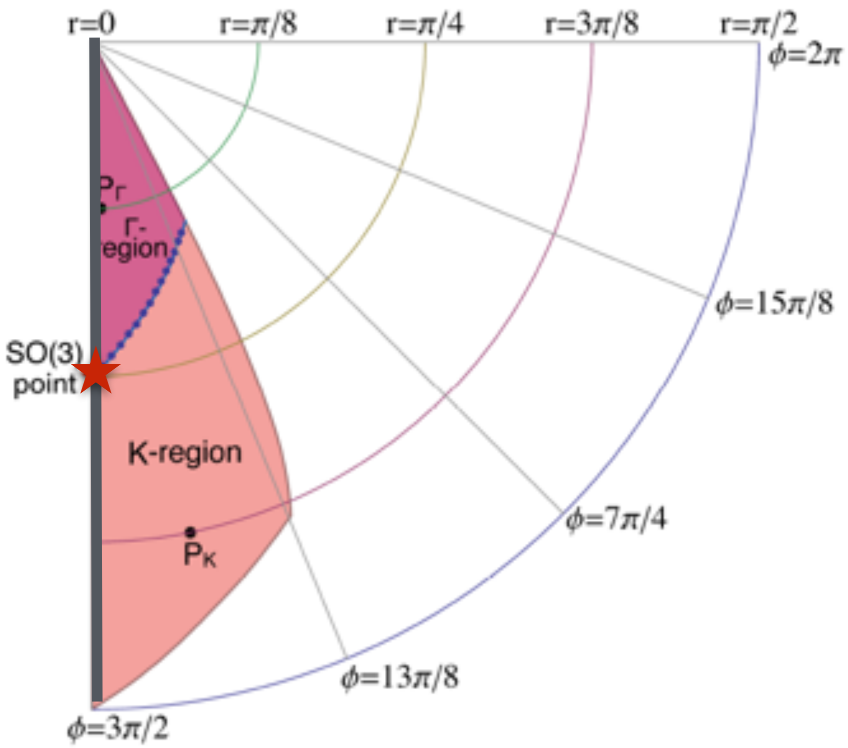

Hidden SO(3) symmetry point

$$K = \Gamma$$

each separate chain

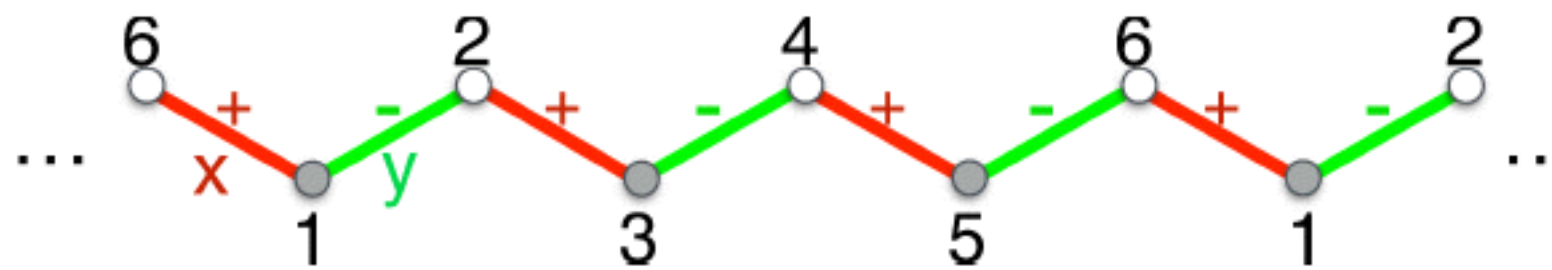

Finite J:

$$E_J \propto J(X_0 - Y_0 - Z_0)^2 + \text{constant}$$

site index j	S_j^x	S_j^y	S_j^z
1	$S_1^{x\prime}$	$S_1^{y\prime}$	$S_1^{z\prime}$
2	$S_2^{z\prime}$	$-S_2^{y\prime}$	$S_2^{x\prime}$
3	$-S_3^{z\prime}$	$-S_3^{x\prime}$	$S_3^{y\prime}$
4	$S_4^{y\prime}$	$S_4^{x\prime}$	$-S_4^{z\prime}$
5	$-S_5^{y\prime}$	$S_5^{z\prime}$	$-S_5^{x\prime}$
6	$-S_6^{x\prime}$	$-S_6^{z\prime}$	$-S_6^{y\prime}$

$$K(S_1^y S_2^y - S_1^x S_2^z - S_1^z S_2^x) \rightarrow -K\mathbf{S}_1' \cdot \mathbf{S}_2'$$

$$\xrightarrow{\text{dual}} \quad \boxed{K' = \Gamma' = 0} \quad \boxed{J' = -K}$$

Main idea: IC order can be understood as a long-wavelength twisting of a nearby commensurate order. In this case: **Q**=(2/3,0,0)

K-dominant state

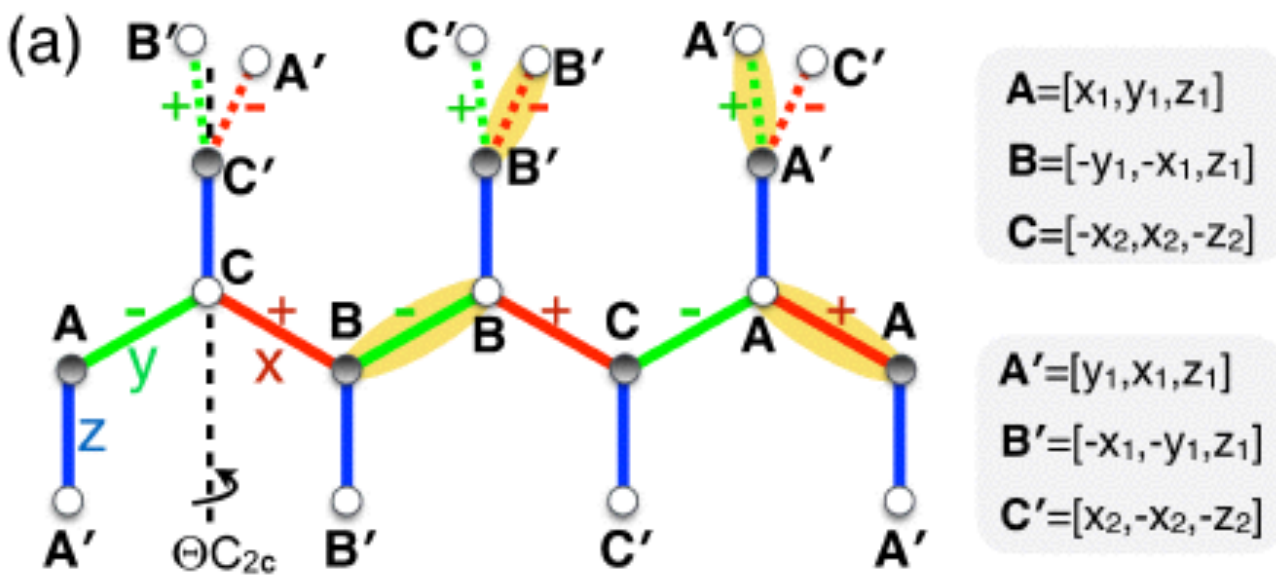

Static structure factor components

Q=2/3: $M_a(A)$, $M_b(C)$ and $M_c(F)$

Γ_4 IRR

Q=0: $M'_a(G)$ and $M'_b(F)$

$$A=\begin{pmatrix}1\\-1\\-1\\1\end{pmatrix},\quad C=\begin{pmatrix}1\\1\\-1\\-1\end{pmatrix},\quad F=\begin{pmatrix}1\\1\\1\\1\end{pmatrix},\quad G=\begin{pmatrix}1\\-1\\1\\-1\end{pmatrix}$$

Six sublattices (A,B,C) and (A’,B’,C’) forming almost ideal 120^o-order

Q=0 canting due M’$_a$(G) and M’$_b$(F)

The counter-rotating along xy- and x’y’chains:
lower spins ABCABC… upper spins ACBACB

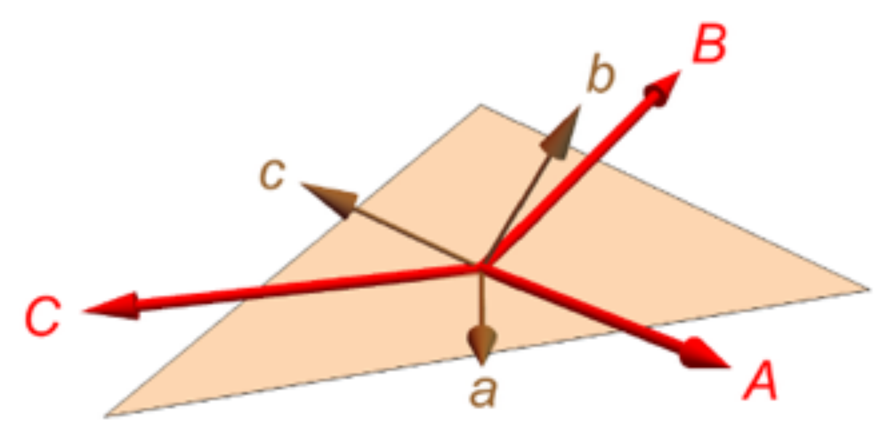

S. Ducatman, I. Rousochatzakis and **N.P.**, PRB 2018

The behavior of β-Li_2IrO_3 *under magnetic field along any crystallographic direction can be described in a unified manner.*

$$\mathcal{H}_{ij}^{t} = J\mathbf{S}_i \cdot \mathbf{S}_j + KS_i^{\alpha_t} S_j^{\alpha_t} + \sigma_t \Gamma (S_i^{\beta_t} S_j^{\gamma_t} + S_i^{\gamma_t} S_j^{\beta_t})$$
$$\mathcal{H}^{Z} = -\mu_B \mathbf{H} \cdot \textstyle\sum_i \mathbf{g}_i \cdot \mathbf{S}_i \, .$$

$$\mathbf{g}_i = \mathbf{g}_{\text{diag}} + p_i \mathbf{g}_{\text{off-diag}} \equiv \begin{pmatrix} g_{aa} & 0 & 0 \\ 0 & g_{bb} & 0 \\ 0 & 0 & g_{cc} \end{pmatrix} + p_i \begin{pmatrix} 0 & g_{ab} & 0 \\ g_{ab} & 0 & 0 \\ 0 & 0 & 0 \end{pmatrix}$$

$$g_{aa} = g_{bb} = g_{cc} = 2$$
$$g_{ab} = 0.1$$

General structure of the field-induced phases

field direction	H‖a					H‖b					H‖c				
Hamiltonian $\mathcal{H}$	$\mathcal{T}$	$\mathcal{I}$	C_{2a}	ΘC_{2b}	ΘC_{2c}	$\mathcal{T}$	$\mathcal{I}$	ΘC_{2a}	C_{2b}	ΘC_{2c}	$\mathcal{T}$	$\mathcal{I}$	ΘC_{2a}	ΘC_{2b}	C_{2c}
state at $0 \leq H < H^*$	×	√	×	×	√	×	√	√	√	√	×	√	√	×	×
state at $H^* < H < H^{**}$	√	√	√	√	√	√	√	√	√	√	√	√	√	×	×
state at $H > H^{**}$	√	√	√	√	√	√	√	√	√	√	√	√	√	√	√

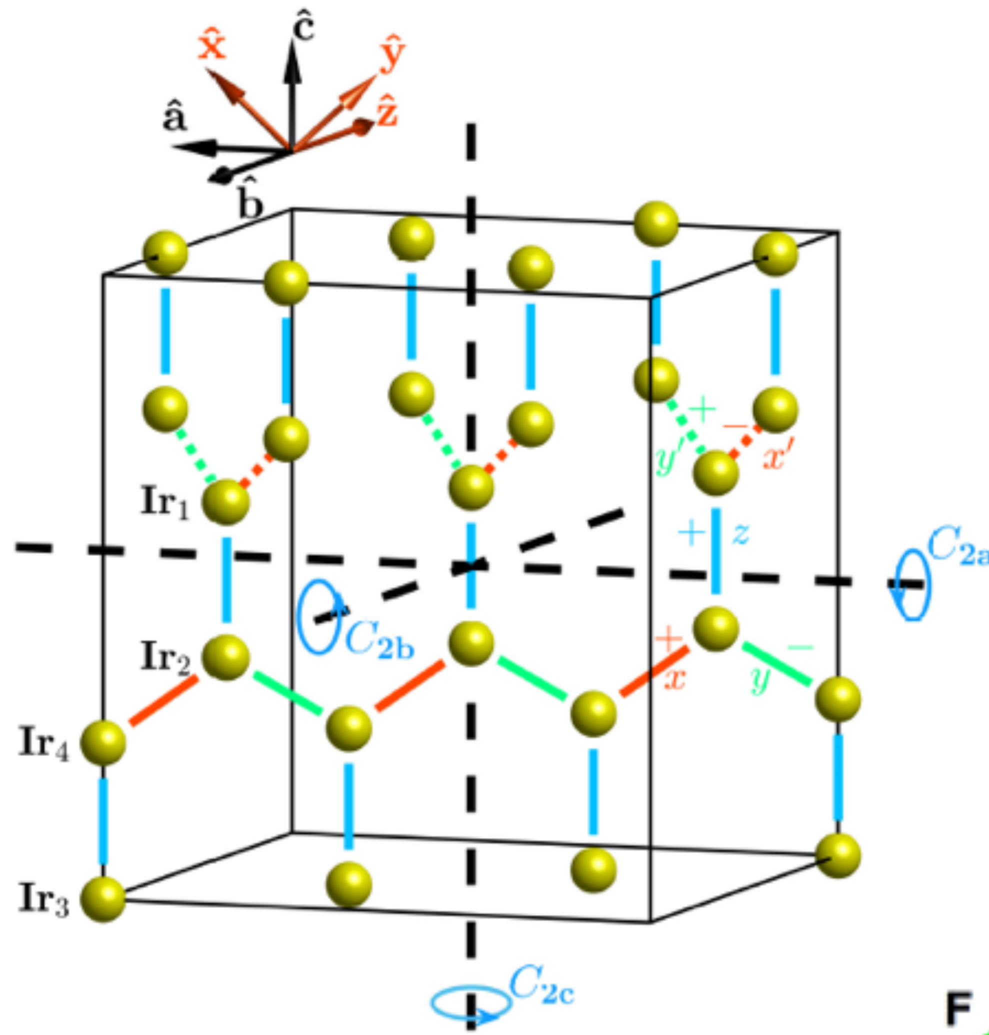

$0 < H < H^*$

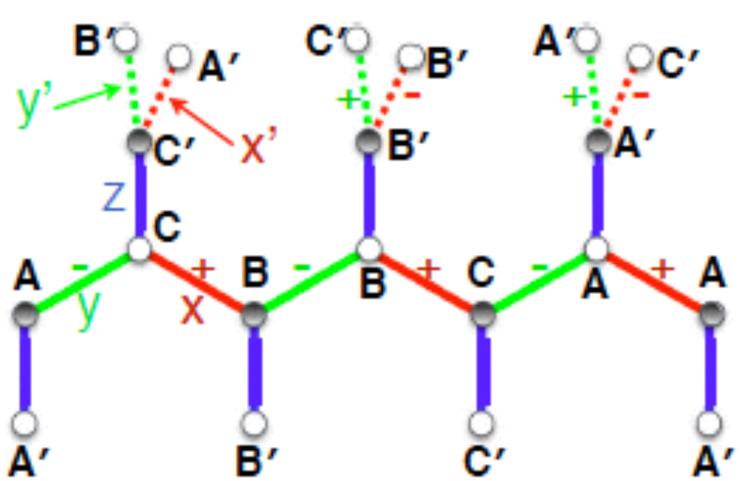

Six-sublattice low-field phase

$H^* < H < H^{**}$

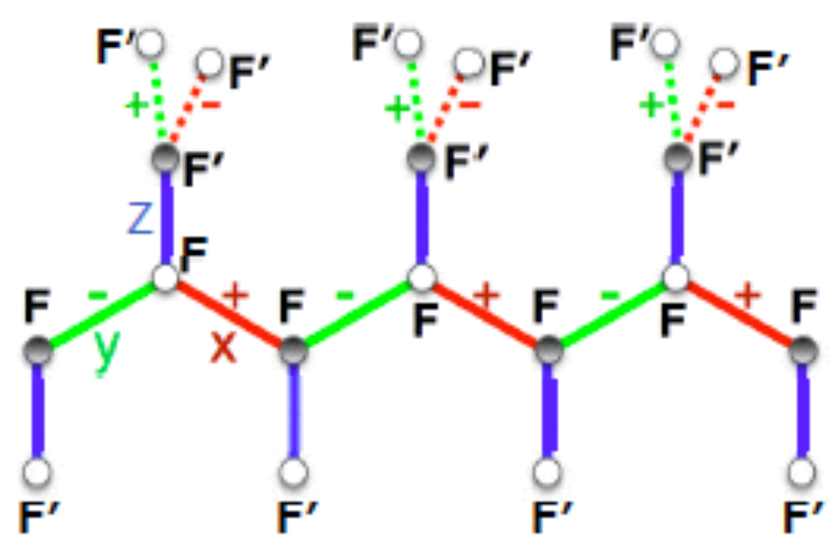

Two-sublattice high-field phase

Symmetries

field direction	H‖a					H‖b					H‖c				
Hamiltonian $\mathcal{H}$	$\mathcal{T}$	$\mathcal{I}$	$C_{2\mathrm{a}}$	$\Theta C_{2\mathrm{b}}$	$\Theta C_{2\mathrm{c}}$	$\mathcal{T}$	$\mathcal{I}$	$\Theta C_{2\mathrm{a}}$	$C_{2\mathrm{b}}$	$\Theta C_{2\mathrm{c}}$	$\mathcal{T}$	$\mathcal{I}$	$\Theta C_{2\mathrm{a}}$	$\Theta C_{2\mathrm{b}}$	$C_{2\mathrm{c}}$
state at $0 \le H < H^*$	×	√	×	×	√	×	√	√	√	√	×	√	√	×	×
state at $H^* < H < H^{**}$	√	√	√	√	√	√	√	√	√	√	√	√	√	×	×
state at $H > H^{**}$	√	√	√	√	√	√	√	√	√	√	√	√	√	√	√

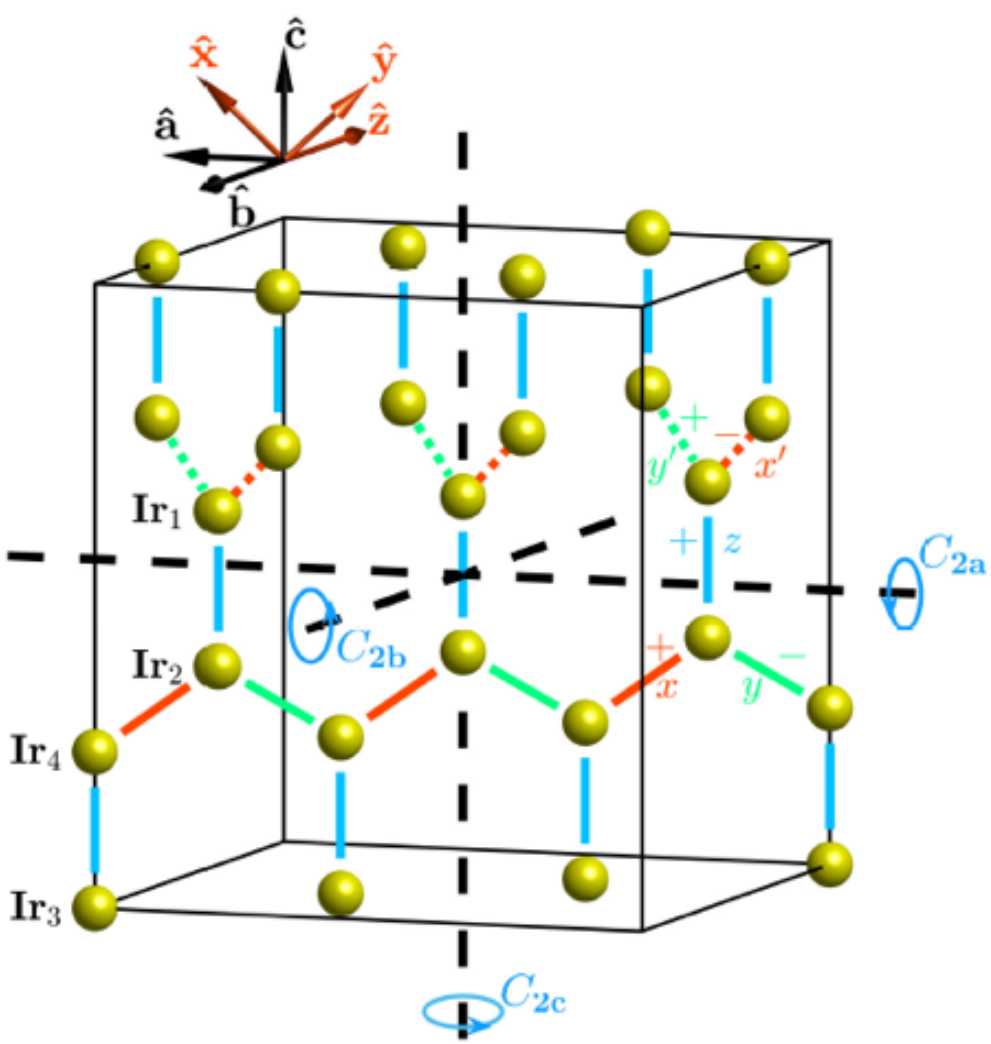

$C_{2\mathrm{c}}$ maps x-bonds to y-bonds
$[S_x, S_y, S_z] \to [S_y, S_x, -S_z]$

$C_{2\mathrm{a}}$ maps x-bonds to y'-bonds and y-bonds to x'
$[S_x, S_y, S_z] \to [-S_y, -S_x, -S_z]$

$C_{2\mathrm{b}}$ maps x-bonds to x'-bonds and y-bonds to y'
$[S_x, S_y, S_z] \to [-S_x, -S_y, S_z]$

Magnetization process in the **b**-field

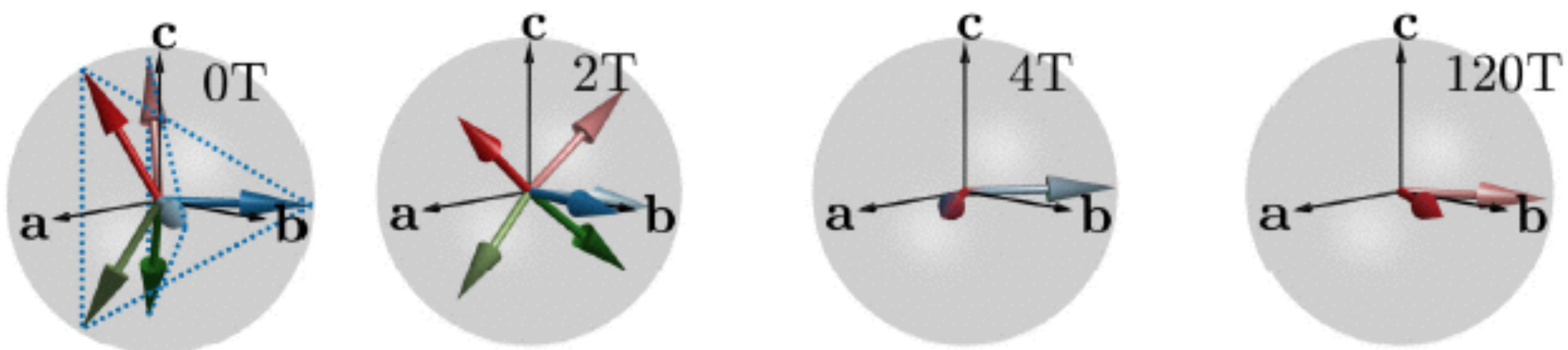

$\boxed{H_{\mathbf{b}}^{*} \sim 2.88\ \mathrm{T}}$ $\boxed{\mu_B H_{\mathbf{b}}^{*} \simeq 0.42 J \left(\frac{4S}{g_{bb}}\right)}$

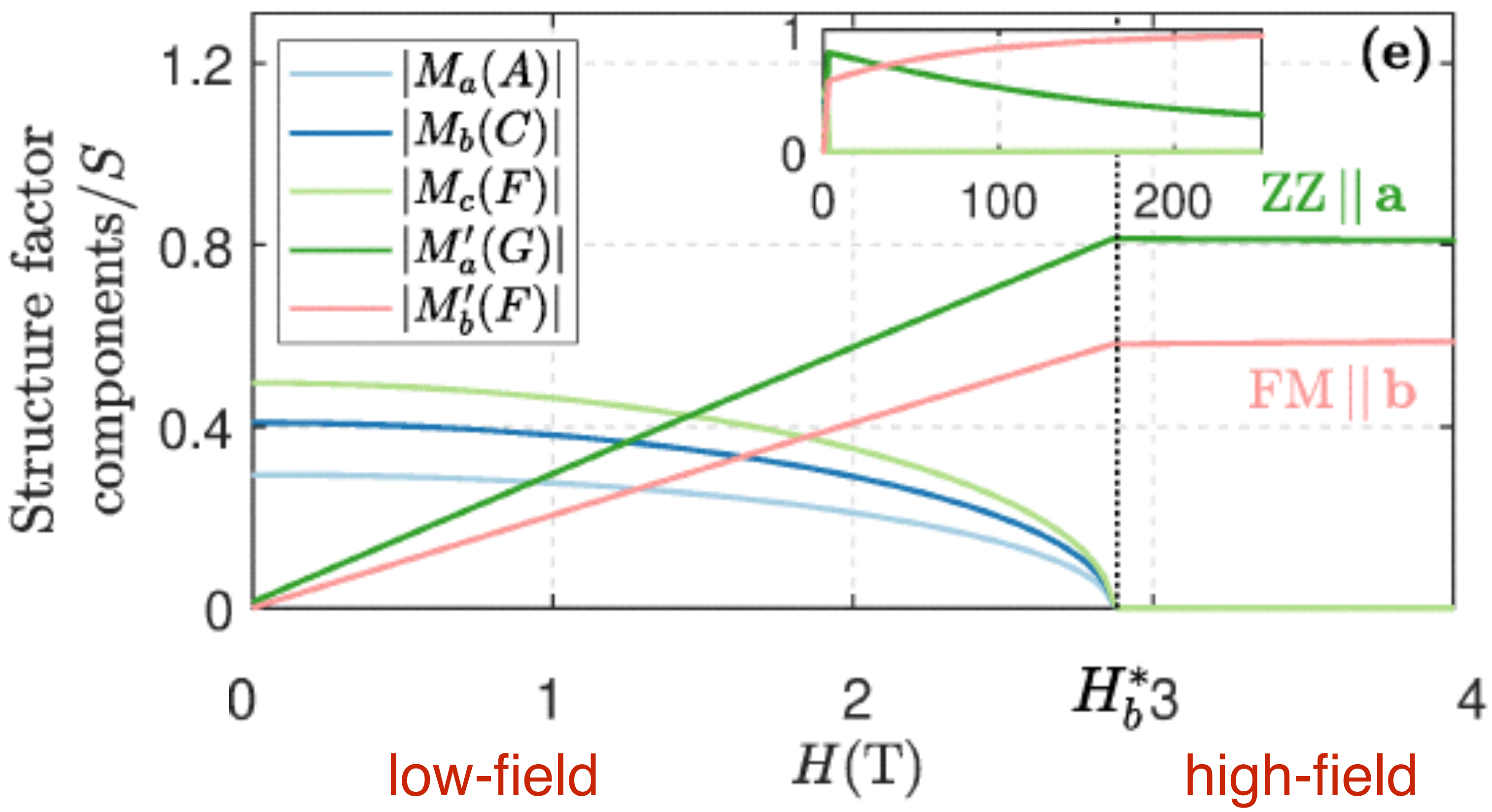

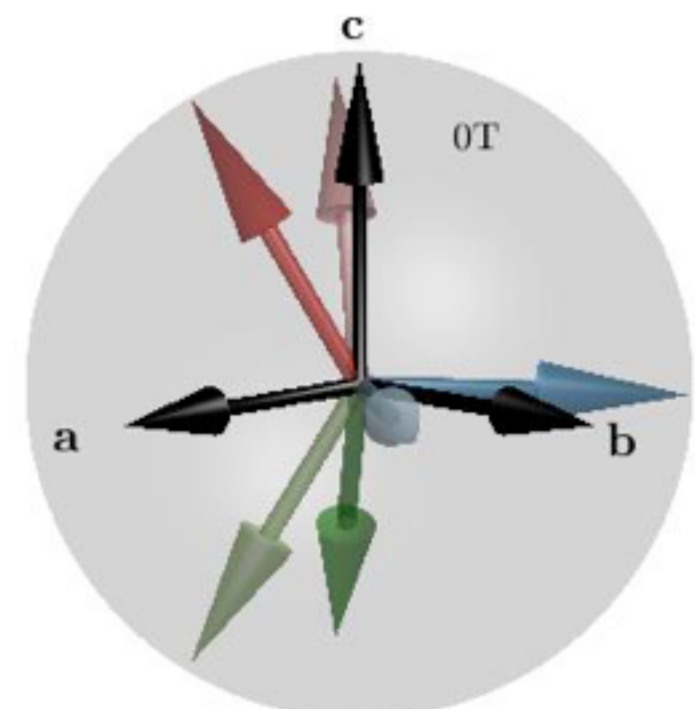

For H > H*, all modulated components vanish and only uniform structure factors left.
Significant zigzag component perpendicular to the field up to very high field, thus the system can not reach fully polarized state even classically.
The spins lie on the ab-plane, so direction of the zigzag is fixed by the field.

Magnetization process in the **a**-field

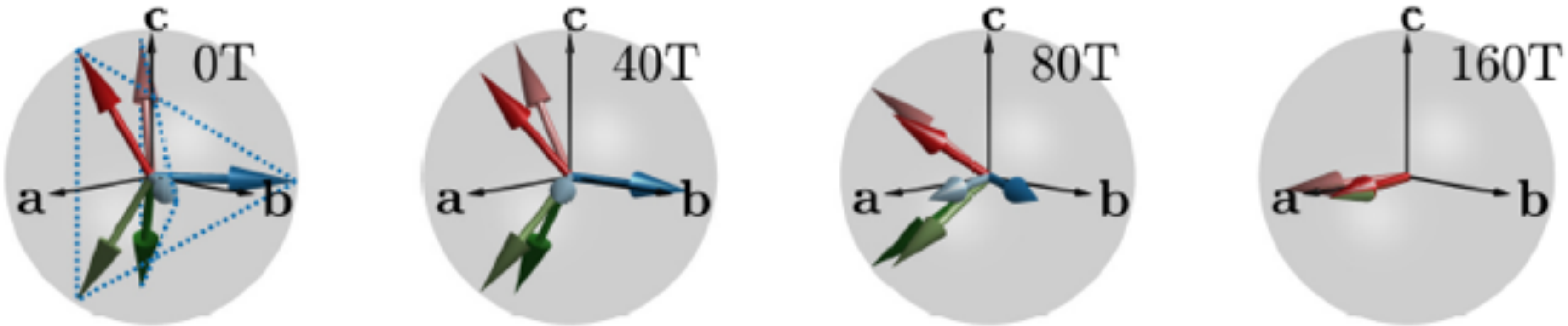

$\boxed{H^*_{\mathbf{a}} \sim 102\ \mathrm{T}}$ $\boxed{\mu_B H^*_{\mathbf{a}} \simeq \left(0.54J + 0.57|\Gamma|\right)\frac{4S}{g_{aa}}}$

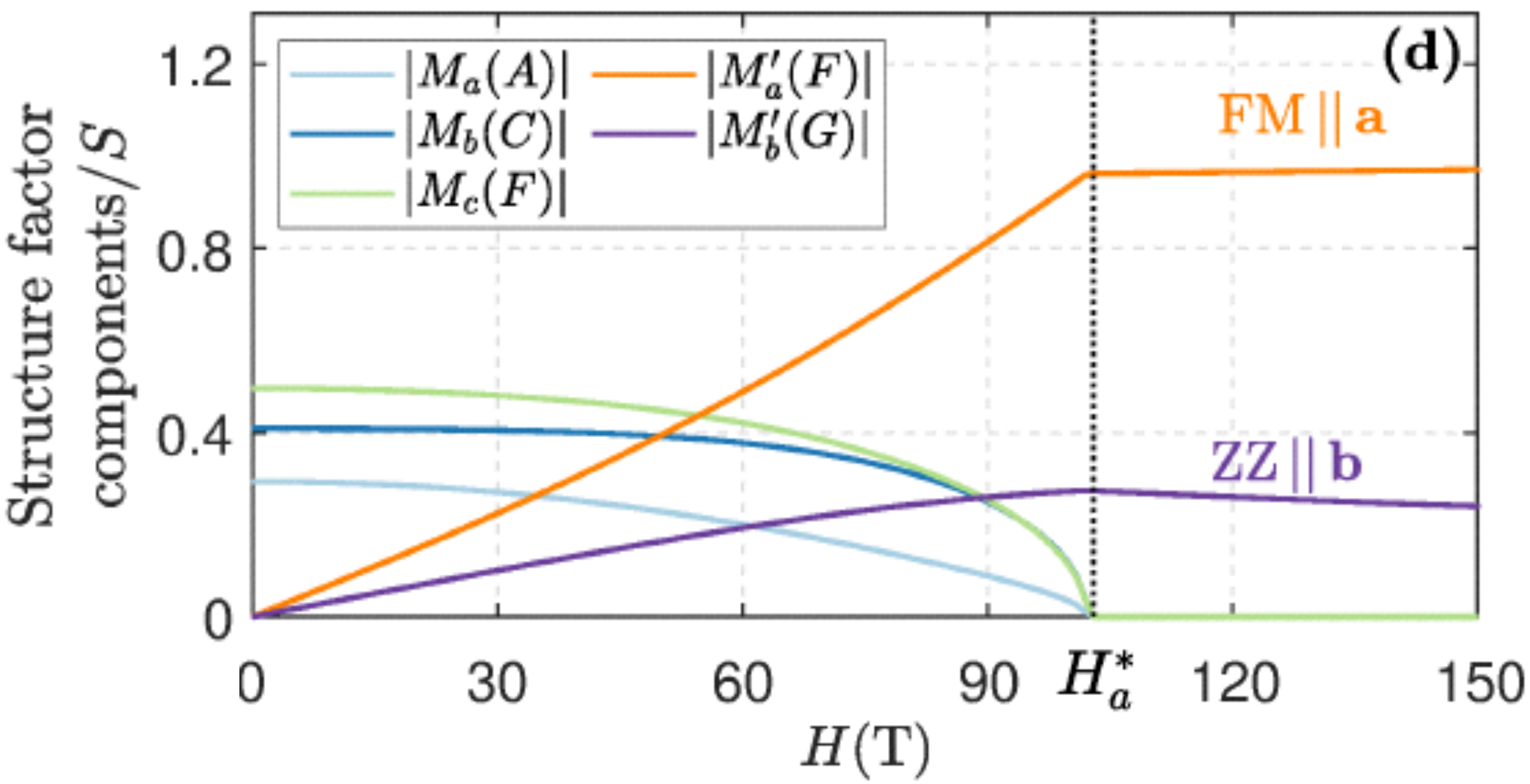

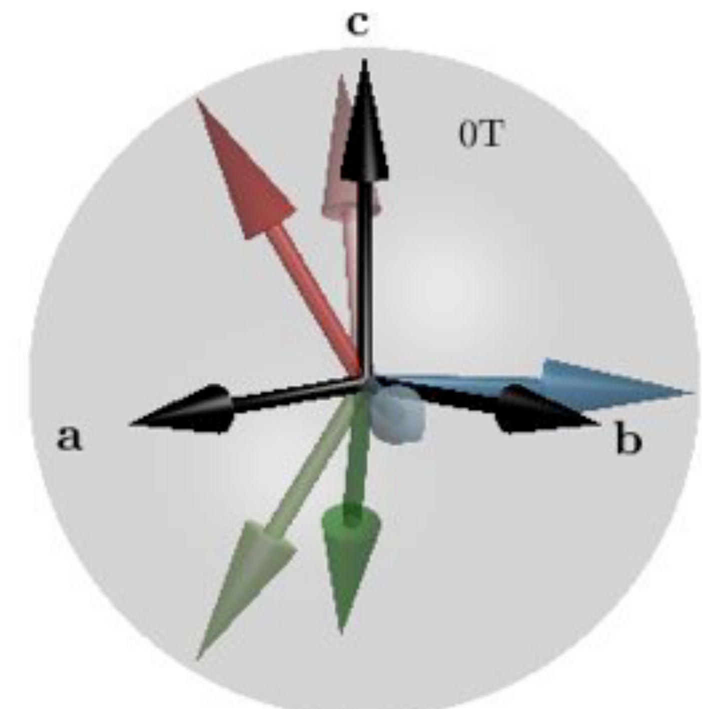

For H > H*, all modulated components vanish and only uniform structure factors left.
Significant zigzag component perpendicular to the field up to very high field, thus the system can not reach fully polarized state even classically.
The spins lie on the ab-plane, so direction of the zigzag is fixed by the field.

Magnetization process in the **c**-field

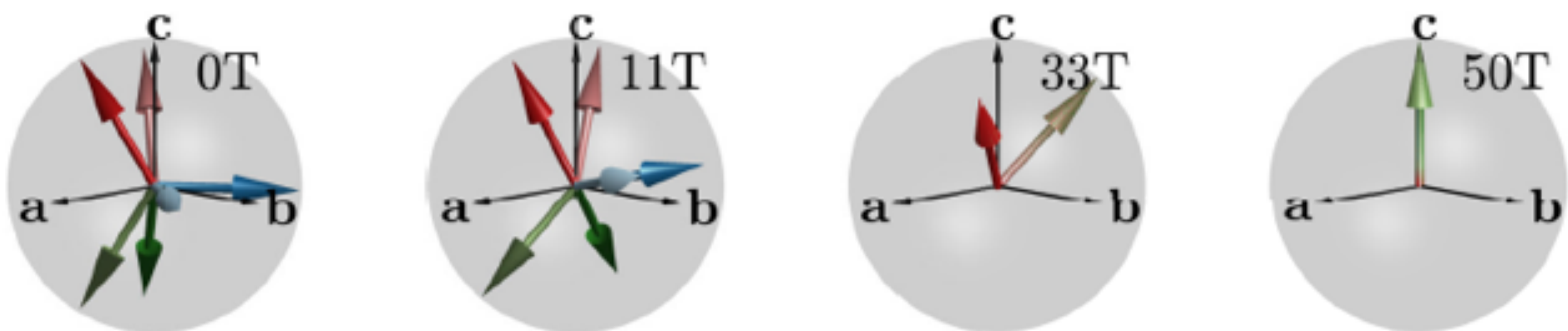

$$\boxed{\mu_B H_{\mathbf{c}}^{**} \simeq \left(\frac{4}{3}J + |\Gamma|\right)\frac{S}{g_{cc}}}$$

$$\boxed{\mu_B H_{\mathbf{c}}^{*} \simeq \left(0.94J + 0.04|\Gamma|\right)\frac{4S}{g_{cc}}}$$

$\boxed{H_{\mathbf{c}}^{*} \sim 13\ \mathrm{T}}$ $\boxed{H_{\mathbf{c}}^{**} \sim 45\ \mathrm{T}}$

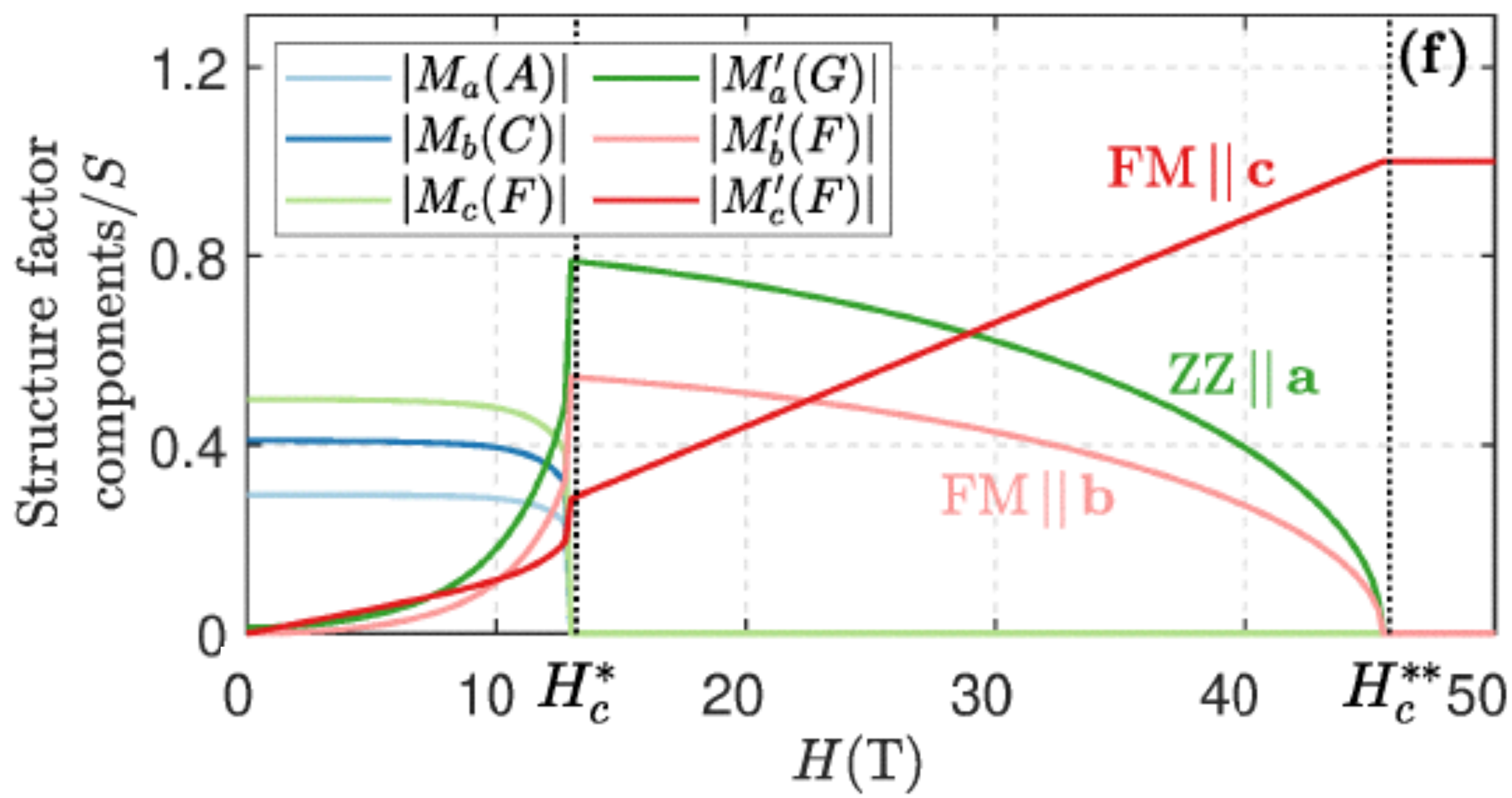

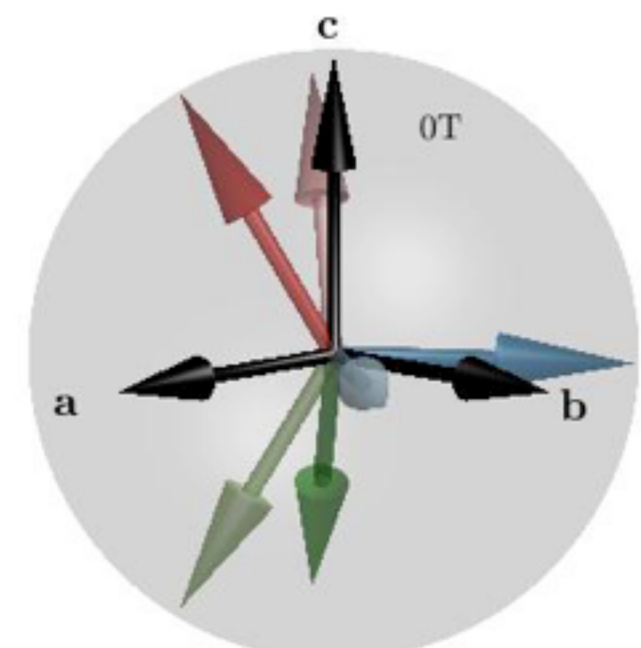

Significant zigzag and additional FM component perpendicular to the field for H > H*. The spin plane changes continuously with a field. However, not all the symmetries are broken and thus there is a second transition at H**. For H>H** the classical system is in a fully polarized state.

Robustness of high-field zigzag orders

$$E_{\mathbf{a}}/N = \eta'_{aF} M'_a(F)^2 + \eta'_{bG} M'_b(G)^2 - \sqrt{2}\Gamma\, M'_a(F)\, M'_b(G)$$
$$- \mu_B H \left(g_{aa} M'_a(F) - g_{ab} M'_b(G) \right) .$$

$$E_{\mathbf{b}}/N = \eta'_{bF} M'_b(F)^2 + \eta'_{aG} M'_a(G)^2 - \sqrt{2}\Gamma\, M'_a(G)\, M'_b(F)$$
$$- \mu_B H [g_{bb} M'_b(F) - g_{ab} M'_a(G)] .$$

$$E_{\mathbf{c}}/N = \eta'_{bF} M'_b(F)^2 + \eta'_{cF} M'_c(F)^2 + \eta'_{aG} M'_a(G)^2$$
$$- \sqrt{2}\Gamma\, M'_a(G)\, M'_b(F) - g_{cc} \mu_B H\, M'_c(F) .$$

The presence of these cross-coupling terms reveal that the qualitative reason why it is energetically favorable for the system to sustain appreciable zigzag orders up to high fields is the strong Gamma- interaction.

Intensity sum rule

A. Ruiz et al, Nat.Com. 2017

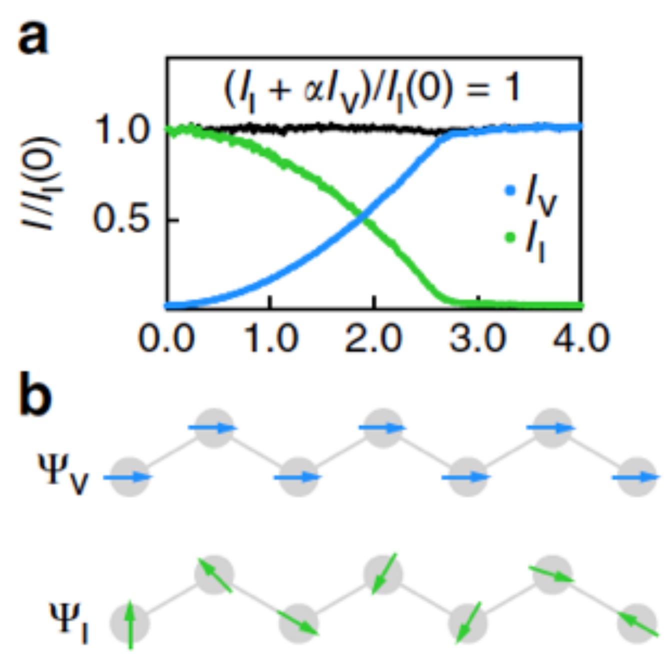

Q=0 order

IC order

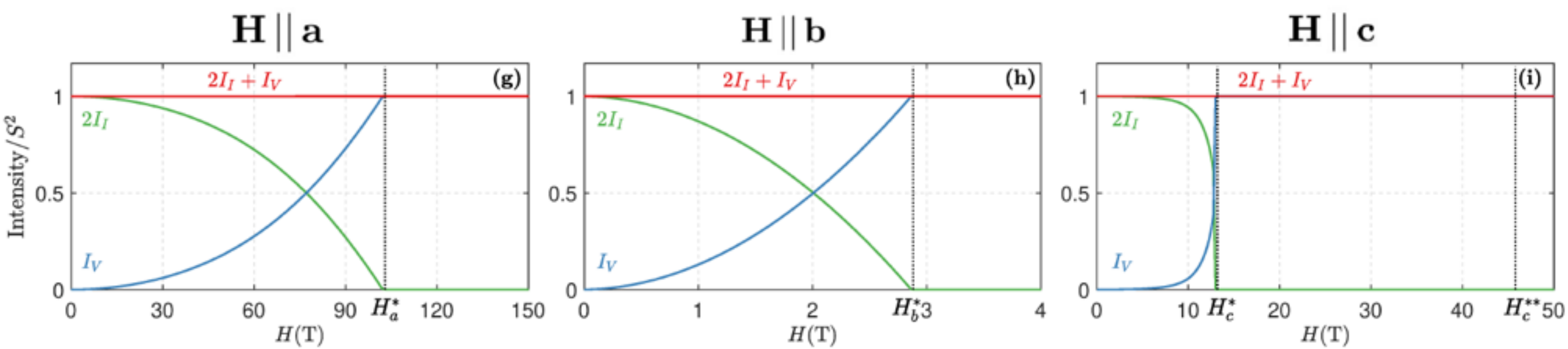

The **intensity sum rule** is fulfilled for **all field directions and strengths**.
This is a direct fingerprint of the local spin length constraints.

Magnetization process

$$\mathbf{m} = \frac{1}{\mathcal{N}_{\mathrm{m}}}\mu_B\left(\mathbf{g}_{\mathrm{diag}} \cdot \sum_{\mu}\langle \mathbf{S}_{\mu}\rangle + \mathbf{g}_{\mathrm{off-diag}} \cdot \sum_{\mu} p_{\mu}\langle \mathbf{S}_{\mu}\rangle\right)$$

$(\mathcal{N}_{\mathrm{m}} = 48 \text{ for } H < H^* \text{ and } \mathcal{N}_{\mathrm{m}} = 2 \text{ for } H > H^*)$

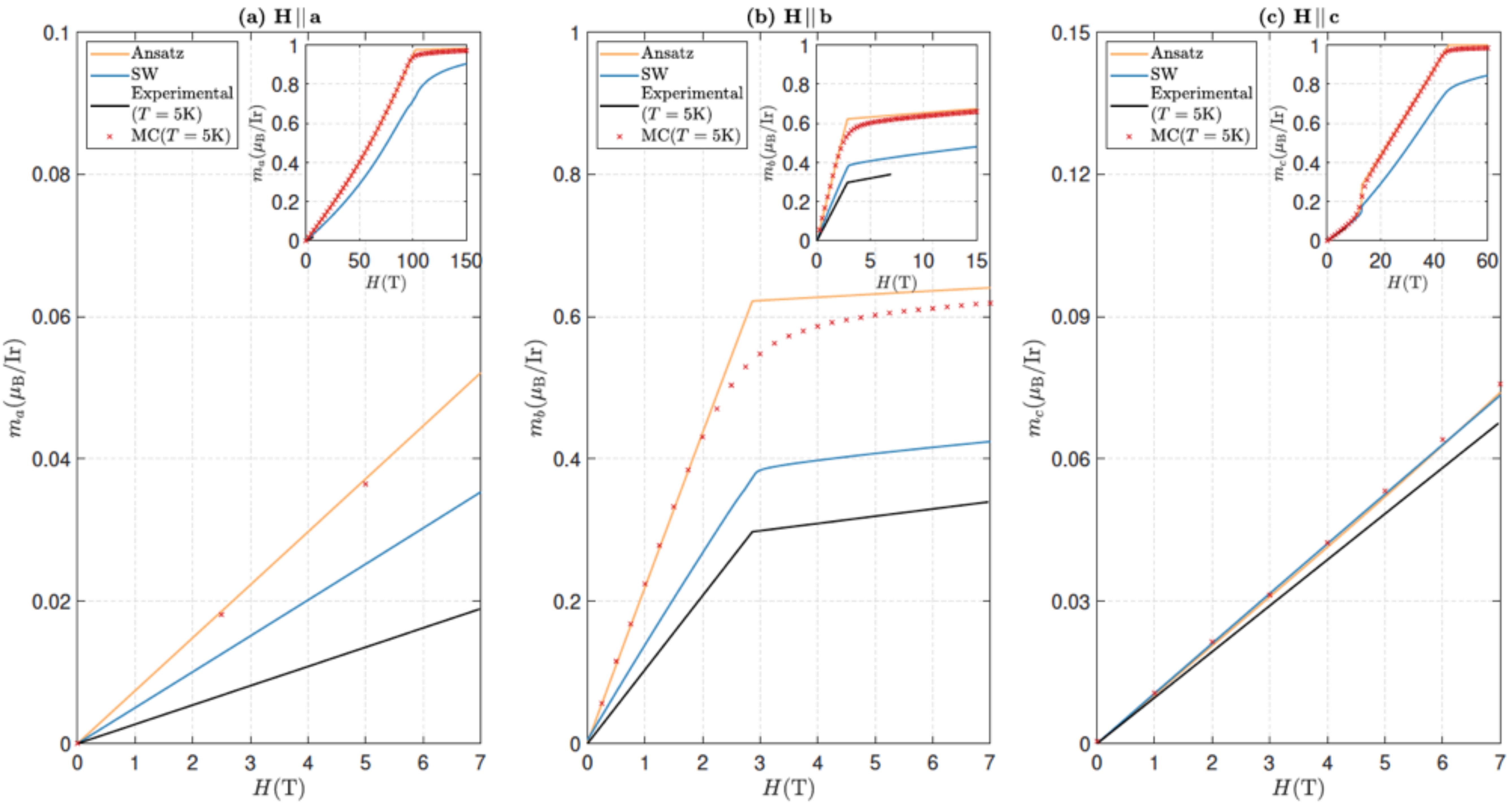

Phase diagram

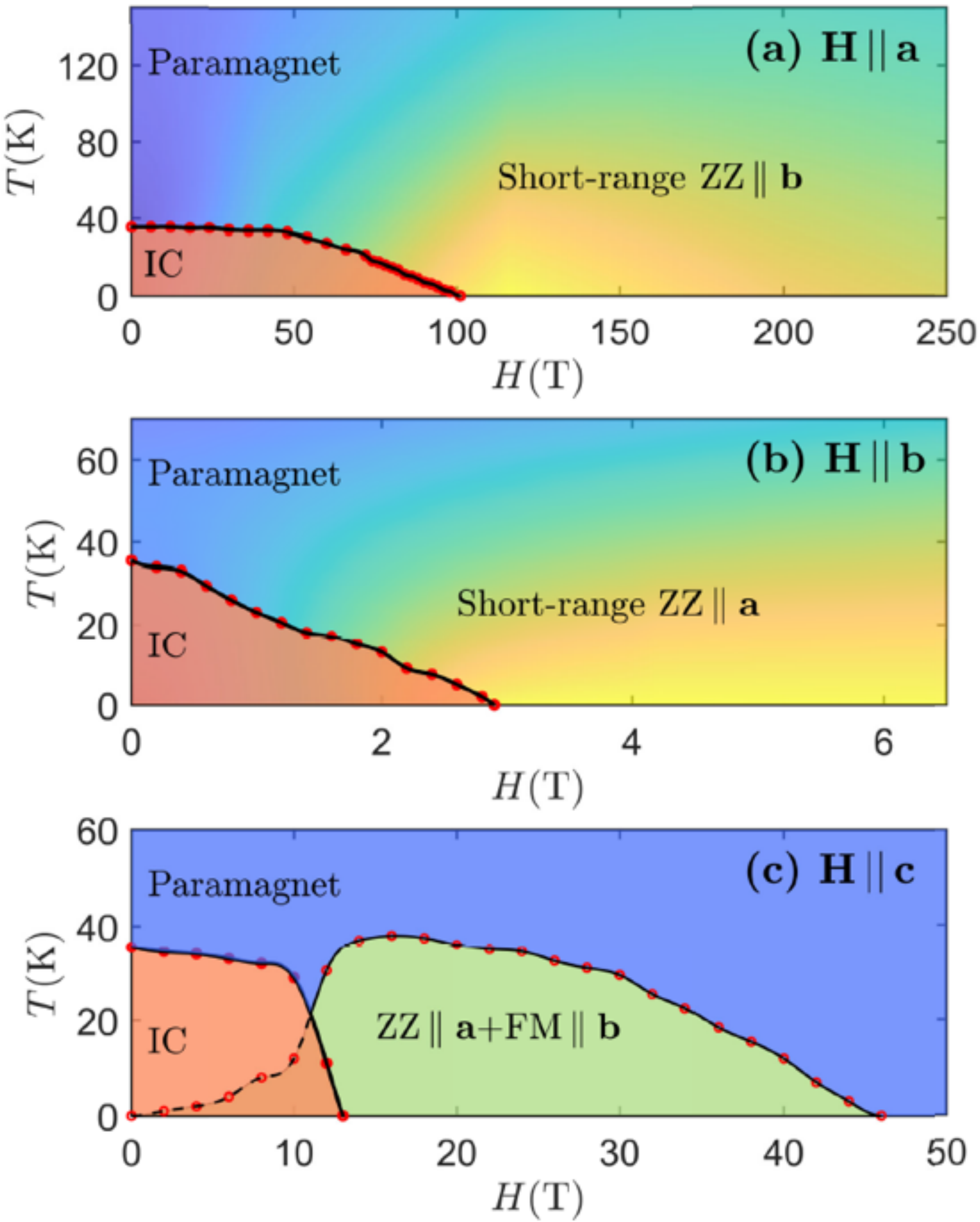

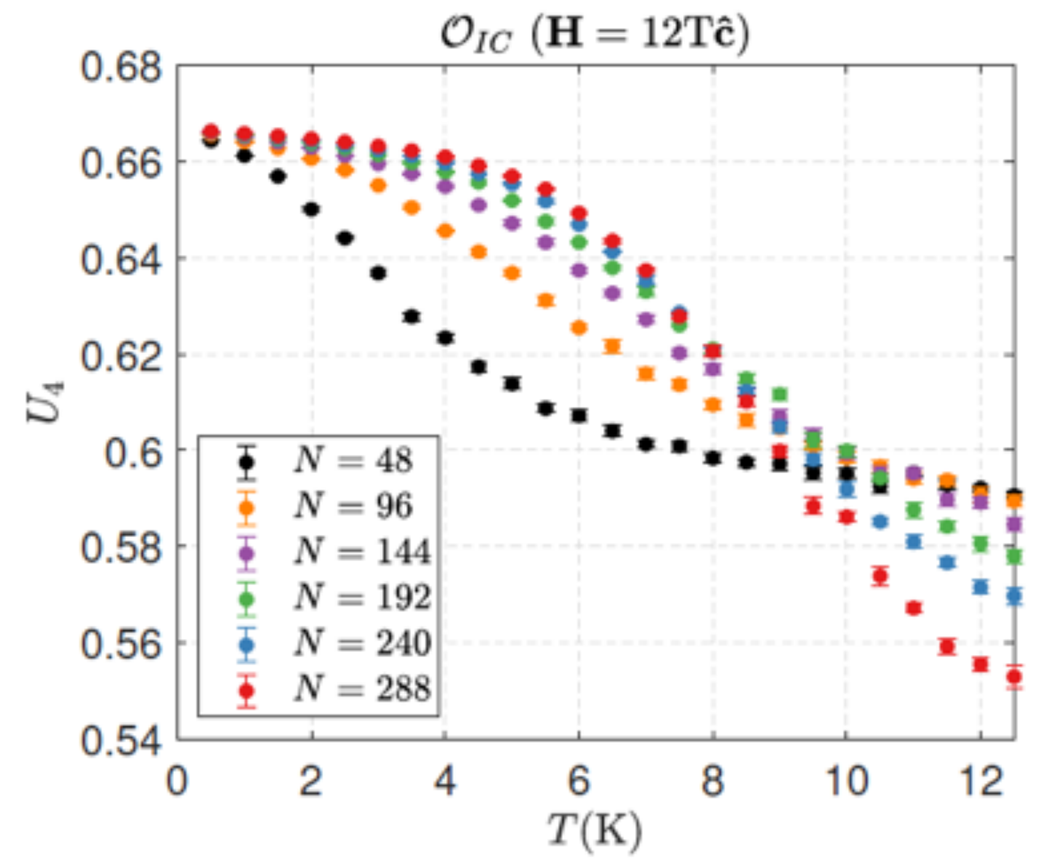

Magnetic excitations in the field

$$\mathcal{H}_2 = E_{cl}/S + \sum \mathbf{x}_\mathbf{q}^\dagger \cdot \mathbf{H}_\mathbf{q} \cdot \mathbf{x}_\mathbf{q}$$

$$\mathbf{x}_\mathbf{q} = \left(a_{\mathbf{q},1}\,, \ldots, a_{\mathbf{q},\mathcal{N}_\mathrm{m}}\,, a^\dagger_{-\mathbf{q},1}\,, \ldots, a^\dagger_{-\mathbf{q},\mathcal{N}_\mathrm{m}}\right)^\mathrm{T}$$

(a) P_K point

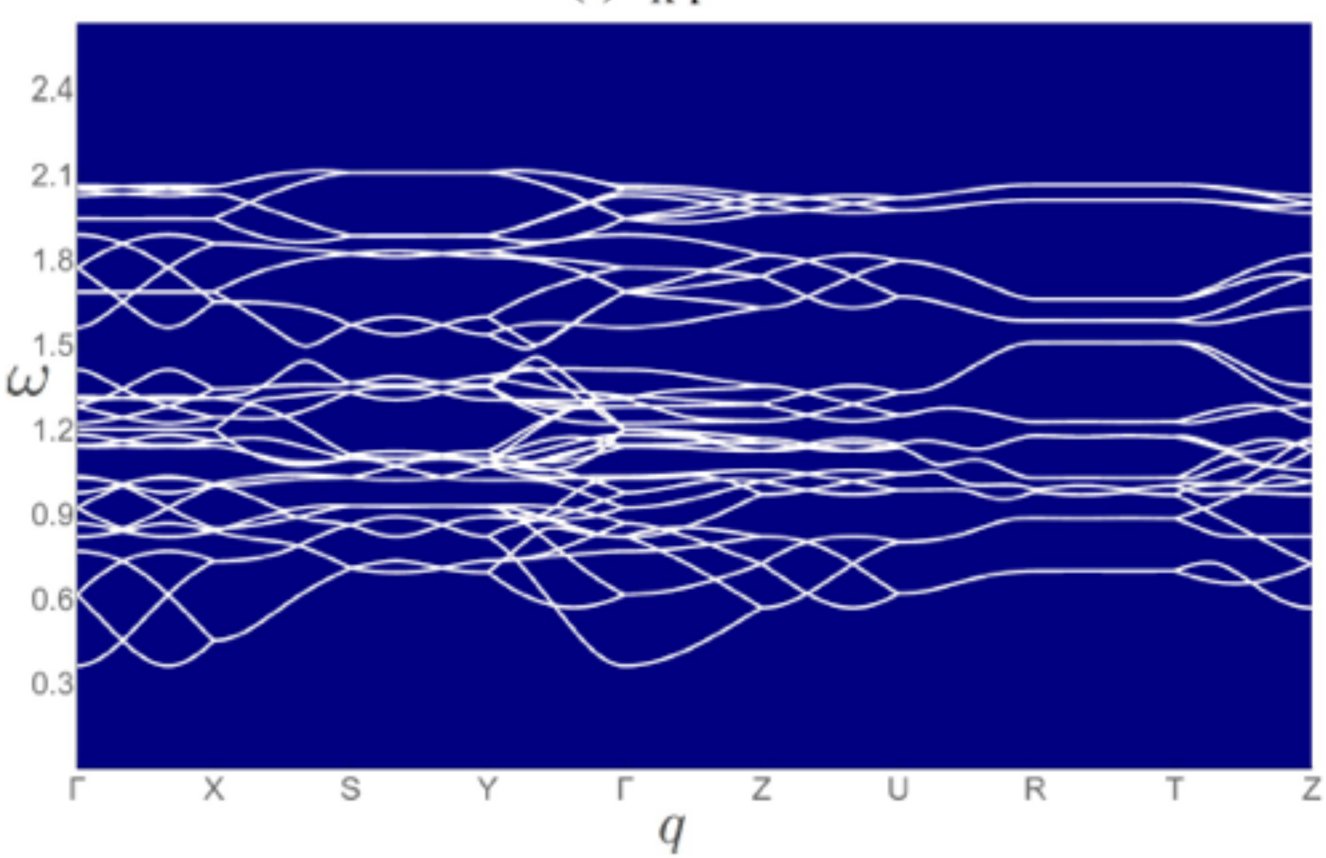

(b) P_Γ point

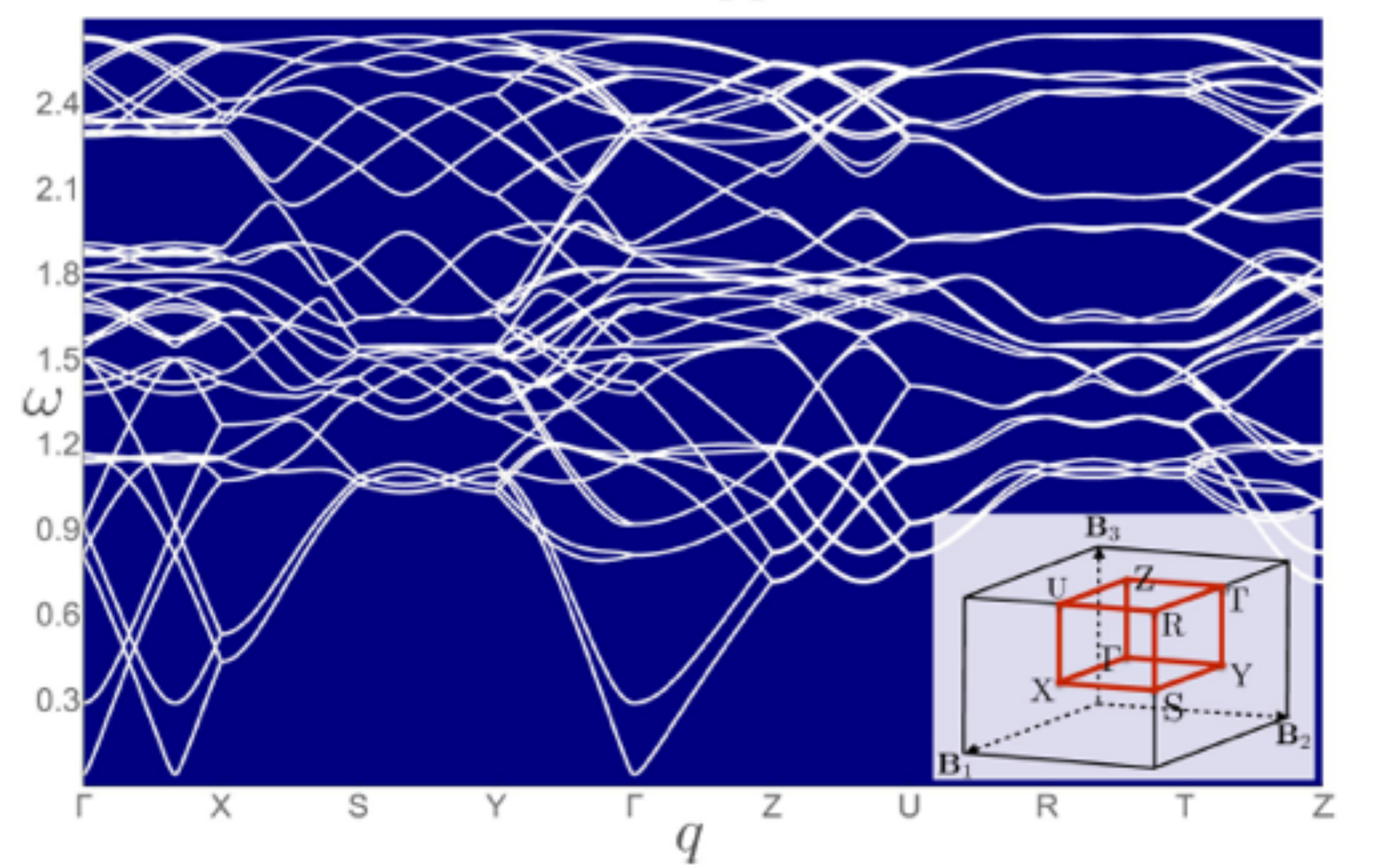

Evolution of magnetic excitations in the b-field

$$I(\mathbf{Q},\omega) \propto \sum_{\alpha,\beta}(\delta_{\alpha,\beta} - \frac{Q^\alpha Q^\beta}{Q^2})S^{\alpha\beta}(\mathbf{Q},\omega)$$

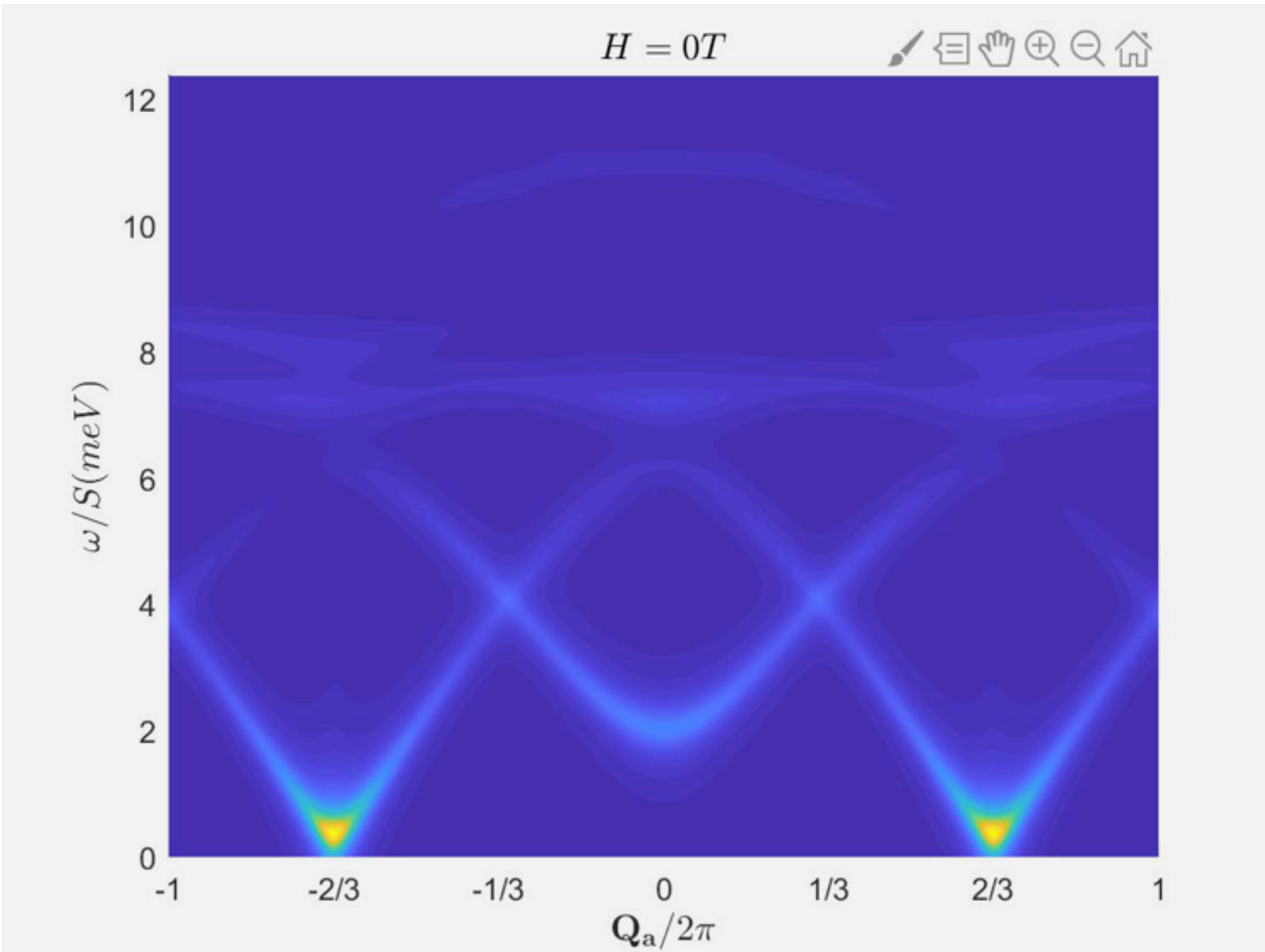

Non-monotonic behavior of spin gap in the b-field

$H < H^*$ the gap decreases as the IC order is being suppressed by the external field;
$H > H^*$ the gap increases and shows a roughly linear behavior indicating that the system is gradually turning into a paramagnet

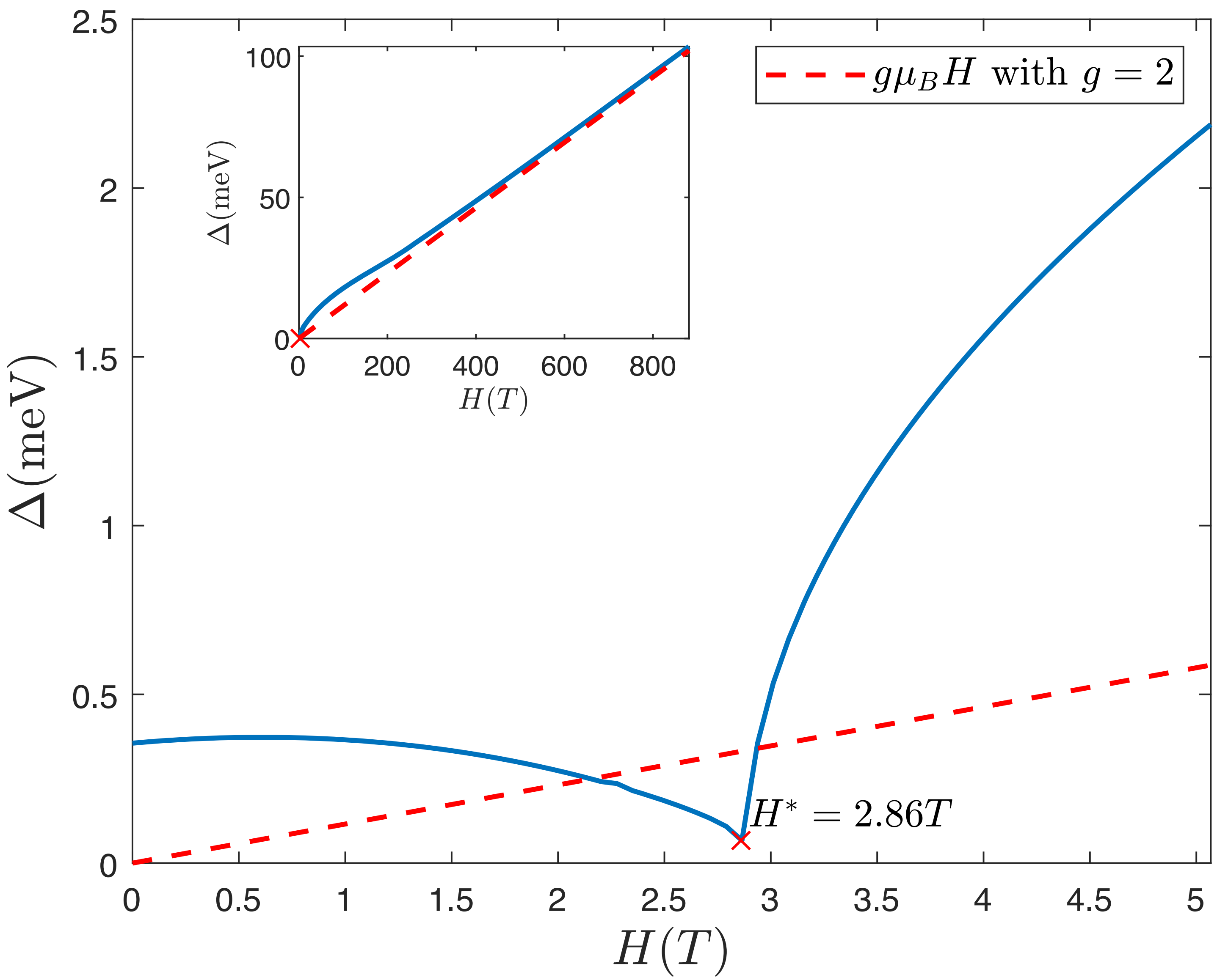

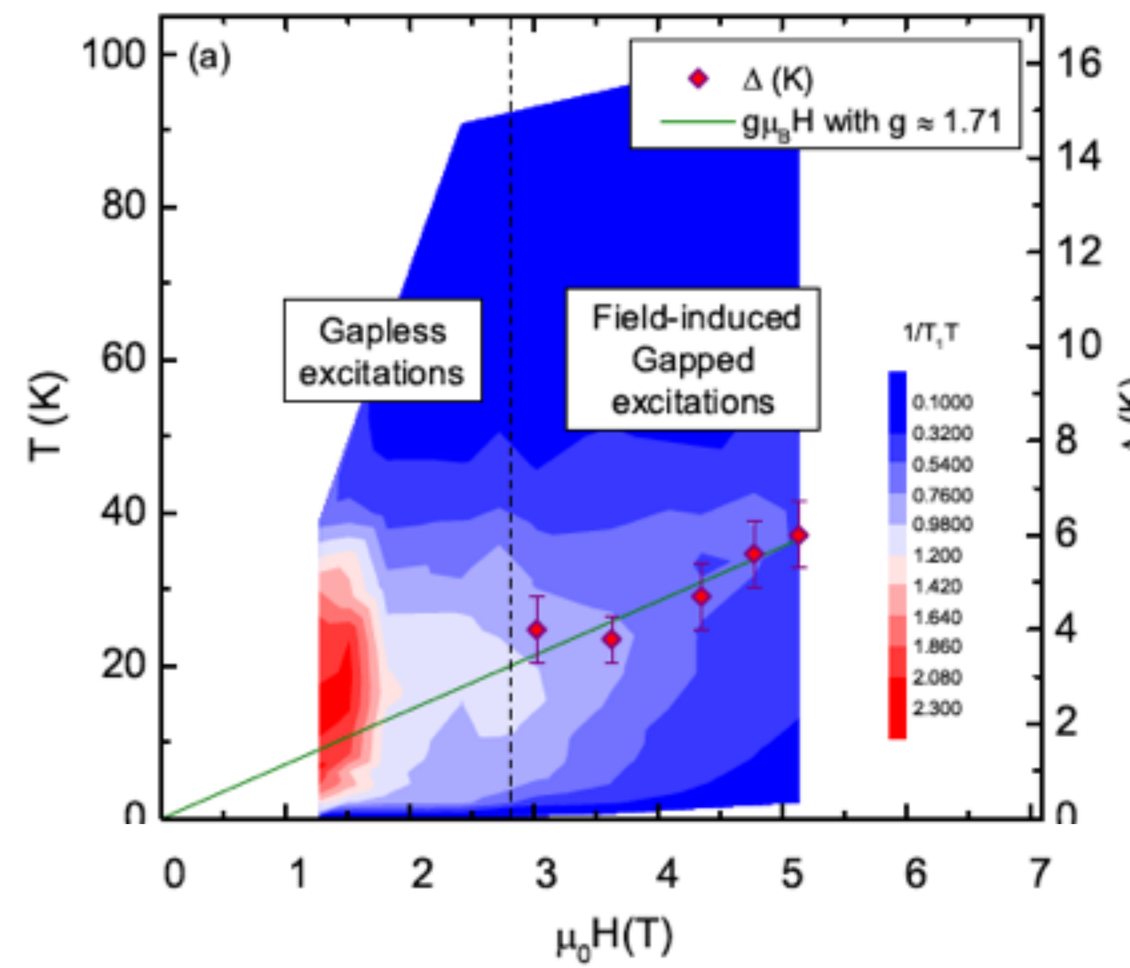

M. Majumder et al, arXiv:1910.03251

Spin gap in the b-field

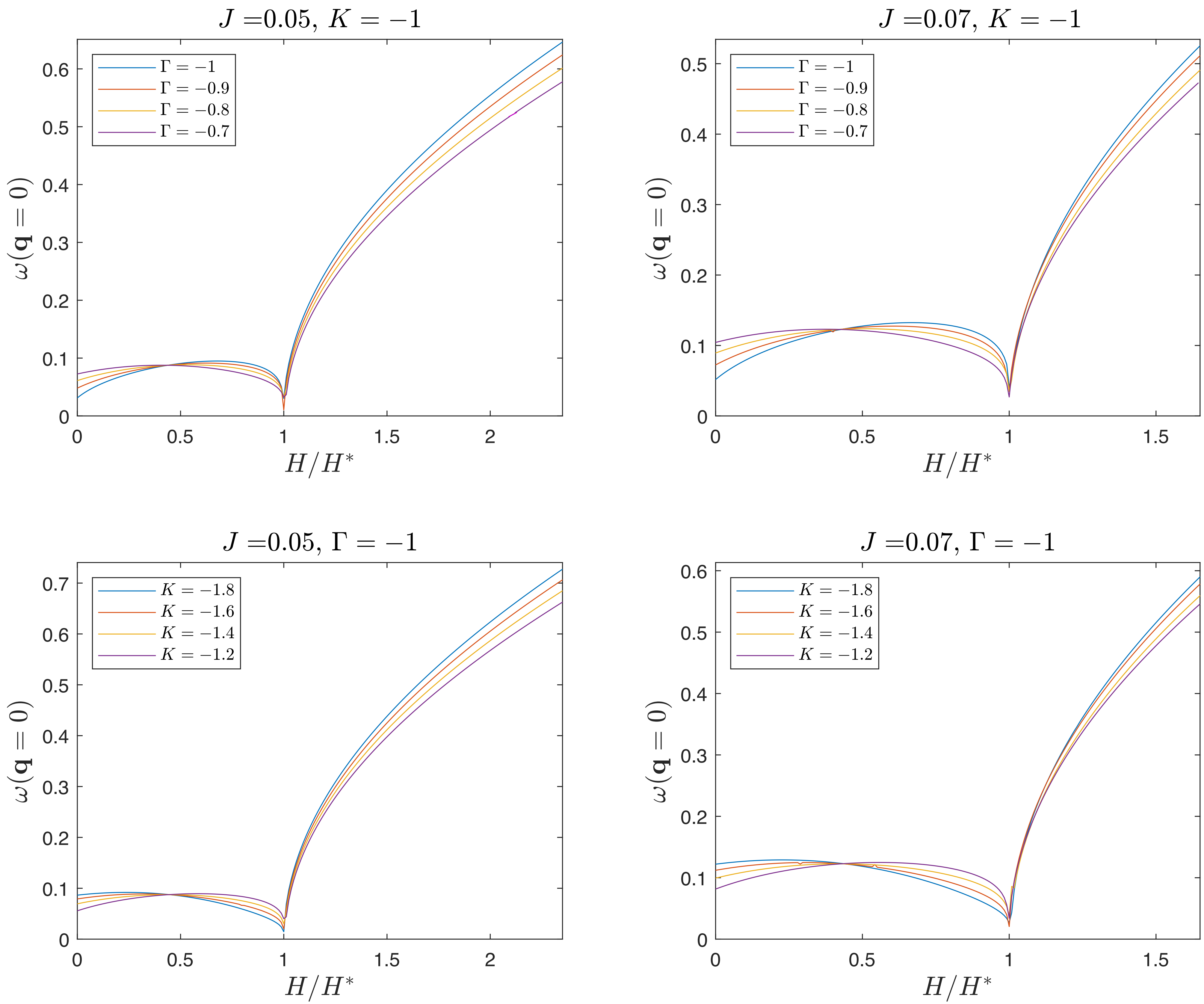

Magnetic torque

$$\mathbf{m}=\begin{cases}[g_{aa}M_a'(F)+g_{ab}M_b'(G)]\hat{\mathbf{a}}+[g_{bb}M_b'(F)+g_{ab}M_a'(G)]\hat{\mathbf{b}}, & \mathbf{H}\,||\,\mathbf{a} \\ [g_{bb}M_b'(F)+g_{ab}M_a'(G)]\hat{\mathbf{b}}, & \mathbf{H}\,||\,\mathbf{b} \\ g_{cc}M_c'(F)\hat{\mathbf{c}}+[g_{bb}M_b'(F)+g_{ab}M_a'(G)]\hat{\mathbf{b}}, & \mathbf{H}\,||\,\mathbf{c}\end{cases}$$

$\mathbf{H}\,||\,\mathbf{a}$: m $\perp$ H $\Rightarrow$ finite torque

$\mathbf{H}\,||\,\mathbf{b}$: zero torque

$\mathbf{H}\,||\,\mathbf{c}$: m $\perp$ H $\Rightarrow$ finite torque

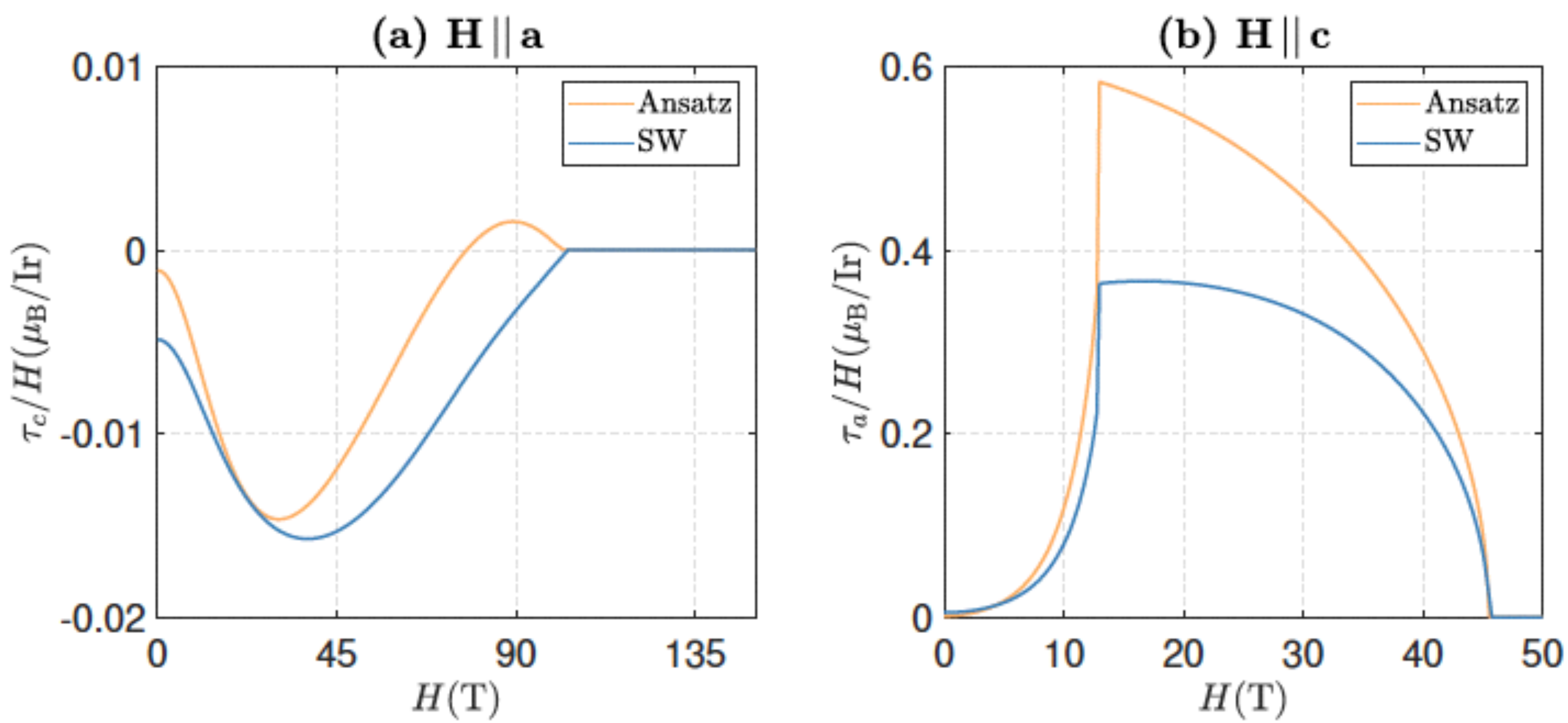

The torque for H II **a** is about 40 times weaker than the torque for H II **c**: $\tau_c \ll \tau_a$

Both torques show a non-monotonic behavior as a function of the field. The kink in τ_a is due to the first-order transition.The sign of τ_a is chosen spontaneously.

Angular dependence of the torque

$$\tau_a/H = -m_c \cos\theta_{bc} + m_b \sin\theta_{bc}$$

$$\tau_c/H = m_a \cos\theta_{ab} - m_b \sin\theta_{ab}$$

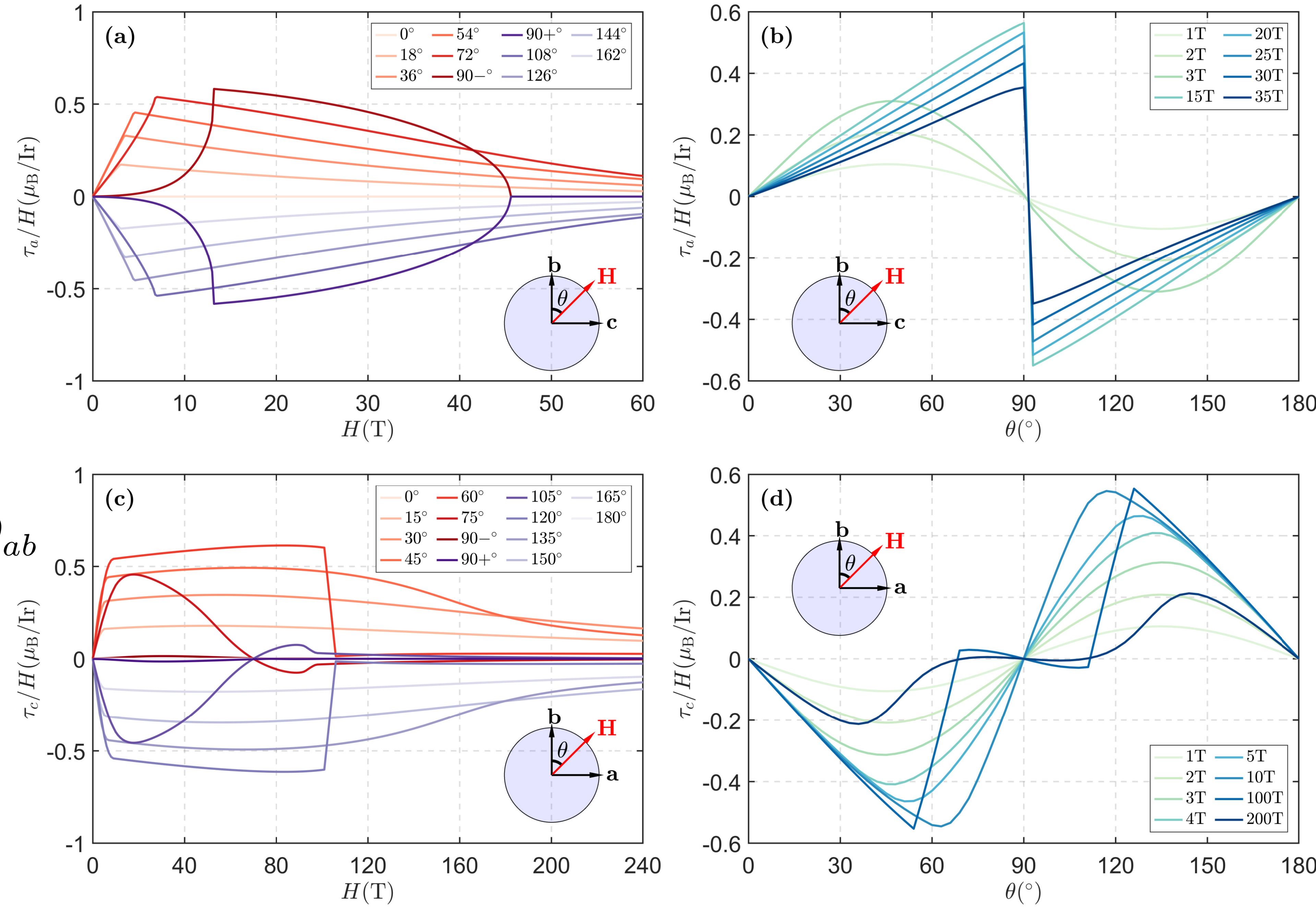

At low fields, the magnetic response is linear and the dependence of the torque is quadratic with field and proportional to sin2θ. Sawtooth shape of the torques for larger fields and angles, comes from the interplay of interaction anisotropy and g-anisotropy.

Also discussed for RuCl3 by K.Riedl, Y. Li, S. M. Winter, and R. Valentí
Phys. Rev. Lett. 122, 197202 2019

Similar angular dependence of the torque was observed in $RuCl_3$ and γ-Li_2IrO_3

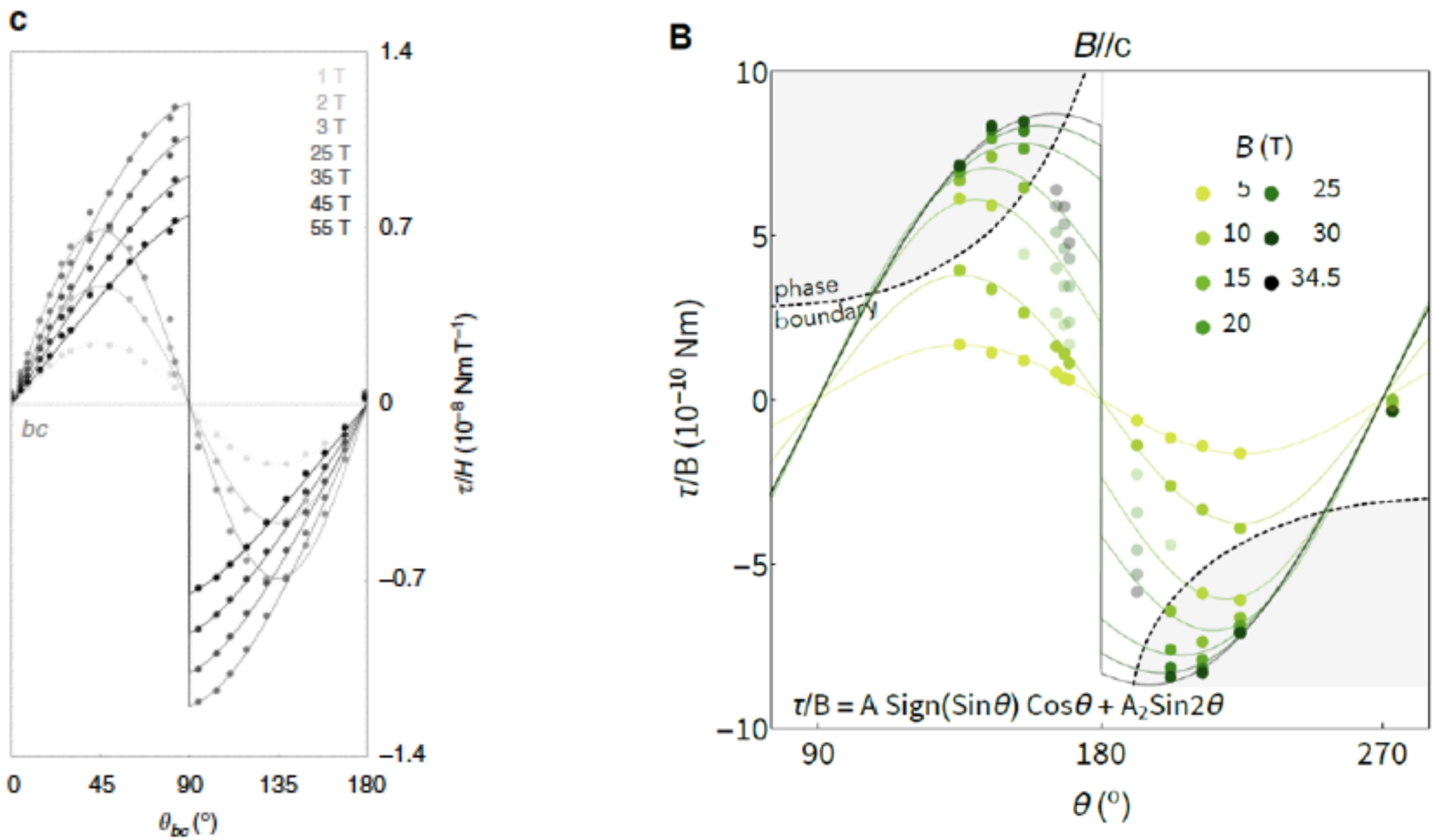

Also discussed for RuCl3 by K.Riedl, Y. Li, S. M. Winter, and R. Val
Phys. Rev. Lett. 122, 197202 2019

Conclusions

zero field:

The period-3 order for dominant K and small J interactions shares the same physics at short distances and the same excitation spectrum with the experimentally observed IC order above some small energy cutoff.

finite field:

Field evolution of the magnetic ground state differs significantly for field along three crystallographic axes due to different symmetry-breaking schemes.

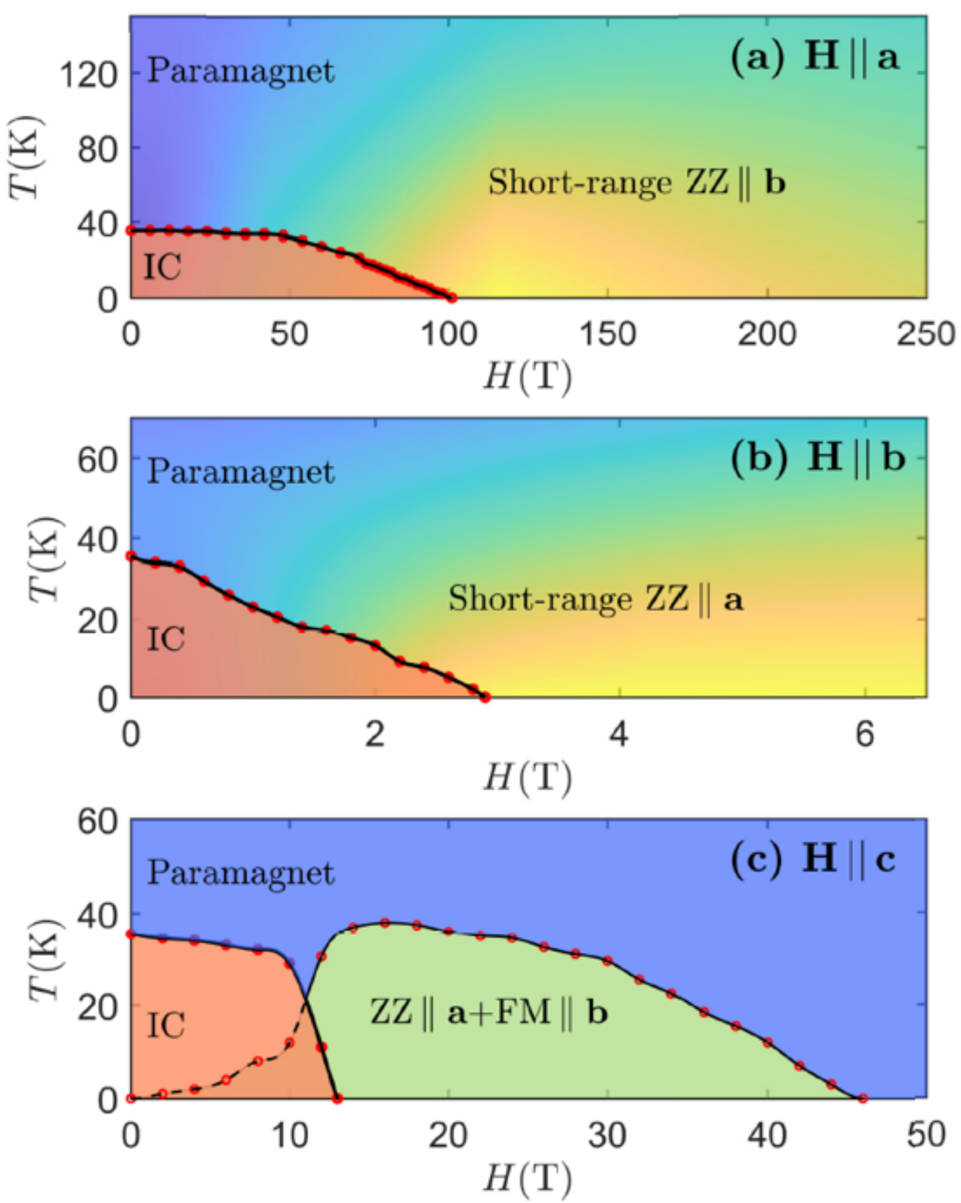

$$\boxed{\mu_B H^*_{\mathbf{a}} \simeq \left(0.54J + 0.57|\Gamma|\right)\frac{4S}{g_{aa}}}$$

$$\boxed{\mu_B H^*_{\mathbf{b}} \simeq 0.42J\ \left(\frac{4S}{g_{bb}}\right)}$$

$$\boxed{\mu_B H^*_{\mathbf{c}} \simeq \left(0.94J + 0.04|\Gamma|\right)\frac{4S}{g_{cc}}}$$

$$\boxed{\mu_B H^{**}_{\mathbf{c}} \simeq \left(\frac{4}{3}J + |\Gamma|\right)\frac{S}{g_{cc}}}$$

Thank you

Ansatz

$\boldsymbol{H//a}$: 10 parameters+ 4 constraints

$$
\begin{aligned}
\mathbf{A} &= S[x_1, y_1, z_1] \\
\mathbf{A}' &= S[y_2, x_2, z_2] \\
\mathbf{B} &= S[-y_1, -x_1, z_1] \\
\mathbf{B}' &= S[-x_2, -y_2, z_2] \\
\mathbf{C} &= S[-x_3, x_3, -z_3] \\
\mathbf{C}' &= S[x_4, -x_4, -z_4]
\end{aligned}
\qquad
\begin{aligned}
x_1^2 + y_1^2 + z_1^2 &= 1 \\
x_2^2 + y_2^2 + z_2^2 &= 1 \\
2x_3^2 + z_3^2 &= 1 \\
2x_4^2 + z_4^2 &= 1
\end{aligned}
$$

$$
\begin{aligned}
E/N = S^2 \Big\{ & K[x_1^2 + x_2^2 + 2x_3y_1 + 2x_4y_2 + 2z_1z_2 + z_3z_4] \\
& + 2\Gamma[x_1x_2 + x_3x_4 + y_1y_2 + x_1z_3 + x_3z_1 + x_2z_4 + x_4z_2 + y_1z_1 + y_2z_2] \\
& + J[2 - 2x_1x_3 - 2x_2x_4 - 2x_3x_4 + 2x_1y_2 + 2x_2y_1 + 2x_3y_1 + 2x_4y_2 + 2z_1z_2 - 2z_1z_3 - 2z_2z_4 + z_3z_4] \Big\}/6 \\
& - \mu_B HS[g^{ab}(-2z_1 + 2z_2 + z_3 - z_4) + \sqrt{2}g^{aa}(x_1 - x_2 - x_3 + x_4 - y_1 + y_2)]/6.
\end{aligned}
$$

$\boldsymbol{H//b}$: 5 parameters+ 2 constraints (same as $\boldsymbol{H} = \mathbf{0}$)

$$
\begin{aligned}
\mathbf{A} &= S[x_1, y_1, z_1] \\
\mathbf{A}' &= S[y_1, x_1, z_1] \\
\mathbf{B} &= S[-y_1, -x_1, z_1] \\
\mathbf{B}' &= S[-x_1, -y_1, z_1] \\
\mathbf{C} &= S[-x_2, x_2, -z_2] \\
\mathbf{C}' &= S[x_2, -x_2, -z_2]
\end{aligned}
\qquad
\begin{aligned}
x_1^2 + y_1^2 + z_1^2 &= 1 \\
2x_2^2 + z_2^2 &= 1
\end{aligned}
$$

$$
\begin{aligned}
E/N = S^2 \Big\{ & K[3 - 2(y_1 - x_2)^2] \\
& + 2\Gamma[1 - z_1^2 + x_2^2 + 2(y_1 + x_2)z_1 + 2x_1z_2] \\
& + J[1 + 2(z_1 - z_2)^2 - 4x_1x_2 + 4(x_1 + x_2)y_1] \Big\}/6 \\
& - \mu_B HS[\sqrt{2}g^{ab}(x_1 - x_2 - y_1) + g^{bb}(-2z_1 + z_2)]/3
\end{aligned}
$$

$\boldsymbol{H//c}$: 9 parameters+ 3 constraints

$$
\begin{aligned}
\mathbf{A} &= S[x_1, y_1, z_1] \\
\mathbf{A}' &= S[y_1, x_1, z_1] \\
\mathbf{B} &= S[-y_2, -x_2, z_2] \\
\mathbf{B}' &= S[-x_2, -y_2, z_2] \\
\mathbf{C} &= S[-y_3, x_3, -z_3] \\
\mathbf{C}' &= S[x_3, -y_3, -z_3]
\end{aligned}
\qquad
\begin{aligned}
x_1^2 + y_1^2 + z_1^2 &= 1 \\
x_2^2 + y_2^2 + z_2^2 &= 1 \\
x_3^2 + y_3^2 + z_3^2 &= 1
\end{aligned}
$$

$$
\begin{aligned}
E/N = S^2 \Big\{ & K[x_1^2 + x_2^2 + z_1^2 + z_2^2 + z_3^2 + 2x_3y_1 + 2y_2y_3] \\
& + \Gamma[x_1^2 + 2x_1z_3 + x_2^2 + 2x_2z_3 + x_3^2 + 2x_3z_2 + y_1^2 + 2y_1z_1 + y_2^2 + 2y_2z_2 + y_3^2 + 2y_3z_1] \\
& + J[(x_1 + y_1)^2 + (x_2 + y_2)^2 - 2x_1y_3 - 2x_2x_3 + 2x_3y_1 + 2y_2y_3 + 2z_1^2 - 2z_1z_3 + 2z_2^2 - 2z_2z_3 + z_3^2 - 2x_3y_3] \Big\}/6 \\
& - \sqrt{2}\mu_B HSg^{cc}(x_1 - x_2 + x_3 + y_1 - y_2 - y_3)/6,
\end{aligned}
$$